

# Uncovering factors to promote high cellulase production with *Thermoascus aurantiacus*

## Author

Lena Victoria Flörl, BSc

## Supervisors

Steven Singer, Ph.D

Raphael Gabriel, Ph.D

(Lawrence Berkeley National Laboratory, California)

Florian Rümer, Ao.Univ.Prof. Dipl.-Ing. Dr.nat.techn.

(University of Natural Resources and Life Sciences, Vienna)

Research Paper for the Austrian Marshall Plan Scholarship

Duration of stay: 29.07.2019 - 14.02.2020

BOKU - UNIVERSITÄT FÜR BODENKULTUR

and

LBNL - LAWRENCE BERKELEY NATIONAL LABORATORY

# Contents

<b>1</b>	<b>Acknowledgments</b>	<b>1</b>
<b>2</b>	<b>Background</b>	<b>2</b>
2.1	Biofuels . . . . .	2
2.2	Enzymatic Cellulose Depolymerization . . . . .	4
2.3	Fungi as expression systems . . . . .	7
2.4	Genetic Manipulation of microbial strains . . . . .	11
2.5	Relevance . . . . .	14
2.6	Strategy and Objective . . . . .	14
<b>3</b>	<b>Material and Methods</b>	<b>15</b>
3.1	Microbiology methods . . . . .	15
3.2	Molecular biology methods . . . . .	18
<b>4</b>	<b>Results and Analysis</b>	<b>24</b>
4.1	Random mutagenesis of <i>T. aurantiacus</i> wild type . . . . .	24
4.2	Sexual crossing results . . . . .	25
4.3	Targeted gene editing of TA using CRISPR-Cas9 . . . . .	29
<b>5</b>	<b>Discussion</b>	<b>35</b>
5.1	Random mutagenesis . . . . .	35
5.2	Sexual crossing . . . . .	36
5.3	CRISPR-Cas9 gene knockouts . . . . .	38
<b>6</b>	<b>Conclusion</b>	<b>42</b>
<b>7</b>	<b>Appendix</b>	<b>43</b>
7.1	Abbreviations . . . . .	43
7.2	Plasmids . . . . .	46
7.3	Media . . . . .	52
7.4	Buffers and solutions . . . . .	53
	<b>References</b>	<b>55</b>

# 1 Acknowledgments

## **Academic supervision and support**

I am thankful to everyone, who supported me during the work on this thesis. I especially acknowledge and express my gratitude to my supervisors Raphael Gabriel, Steven Singer, and Florian Rümer.

I would also like to thank Henrique de Paoli and Joonhoon Kim for their expertise and broad support. Carlos Romereo Vasquez and Pallas Chou were of great help in the lab.

## **Funding sources**

My stay abroad was made possible by the The Marshall Plan Foundation and their generous scholarship program.

The Joint BioEnergy Institute provided me with prime research facilities and materials.

**Thank you!**

## 2 Background

### 2.1 Biofuels

In 2016 representatives of 196 nations negotiated the Paris Climate Agreement to keep the increase in global average temperature below 2 °C – marking international recognition of and effort to tackle globally rising temperatures. Climate change is largely caused by the release of greenhouse gases like CO<sub>2</sub> from the burning of fossil fuels for energy [8]. The transition to carbon free energy sources is nascent and difficult while humanity’s energy consumption increases. There are steps we can take to meet increasing demand, while still reducing carbon footprint.

The Intergovernmental Panel on Climate Change (IPPS) proposes in their report from 2014 that cellulose based feedstocks offer a renewable and carbon neutral fuel source [34, 27]. Additionally they are widely available and compared to petroleum even have a lower cost per unit energy [27]. Biofuels are considered a great opportunity to decrease the reliance on crude petroleum, increase energy security and diversify a countries energy supply [38]. They are expected to stimulate economic growth especially in rural areas and bring thousands of new jobs [38, 27].

The U.S. Department of Energy defines biofuels as transportation fuels made from biomass, which can be plants as well as different types of waste. Liquid biofuels include butanol from fermentation of biomass mainly with *Clostridium*, biodiesel from transesterification of residual fats and oils and bioethanol - which is also considered the most promising drop-in biofuel [38].

#### **Second generation bioethanol**

Contrary to the the first, second generation bioethanol principally is produced from non-food raw material. The used biomass generally is cheap, and readily and locally available [38].

Second generation bioethanol can be based on lignocellulosic biomass, industrial byproducts or wastes. Industrial byproducts could be whey from a dairy which due to the high organic load is expensive to dispose, or glycerol from the biodiesel production. More commonly used though is lignocellulosic biomass from crops growing on poor soil like switchgrass, agricultural and woody wastes like wheat straw and rice husk, or simply from forest biomass [38].

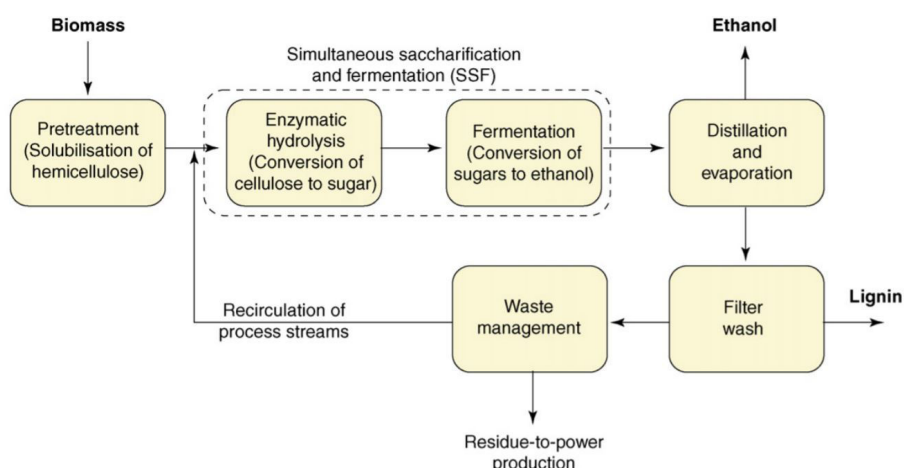


**Figure 2.1.** Schema for the general production of biofuels from lignocellulosic biomass [18]

Lignocellulose based biofuels generate lower levels of net greenhouse gas than the first generation as well as causing less air pollution [18]. But due to the more complex starting material the process to gain fermentable sugars from e.g. wood is also significantly more challenging (see Fig. 2.1 and Chapter 2.2).

The mission of the Joint BioEnergy Institute (JBEI) is to establish new technologies and expand scientific knowledge in the development of feedstock, deconstruction and separation processes, and conversion to carbon-neutral and economically viable biofuels and renewable chemicals. The production of these advanced bioproducts is pursued by a combination of ionic liquid pretreatment, exploration of enzymes and microbes that can deconstruct plant biomass and the metabolic engineering of microbes.

### 2.1.1 Microbial conversion of sugars to biofuels and biochemicals

Two main requirements for microbial strains converting sugars into biofuels or biochemicals are the ability to use all sugars present and to be resistant to possibly cell-toxic or growth-reducing compounds released during biomass degradation. Typical examples thereof are furfural and hydroxymethyl-furfural, a type of dehydrated sugar which is released upon acid pretreatment of biomass and highly toxic to yeast [8].

#### Pretreatment of lignocellulosic biomass

To enhance hydrolysis of cellulose from lignocellulosic biomass it has to be pretreated, which increases accessibility for enzymes or acids and thereby the yield of further fermentable sugars. Several different methods therefore have been developed, including physical milling or grinding,

chemical treatment with acids, bases or organic solvents, combinations of physio-chemical methods like hot water or steam explosion and even some biological methods [24].

Effective pretreatment should decrease the crystalline structure of the comprised cellulose and increase the for enzymes accessible surface area, hemicellulose and/or lignin should be solubilized, while the loss of sugars and the formation of inhibitors should be avoided [24].

Following the pretreatment, the remaining solids are separated from the soluble sugars which are further hydrolyzed by commercially available enzyme mixes [8].

## 2.2 Enzymatic Cellulose Depolymerization

Enzymatic depolymerisation of the highly recalcitrant lignocellulose raw material is still a bottleneck in industrial biofuel production as large amount of enzymes are required, which production in this scale is rather costly [37]. Studies suggest that per dollar spent on biofuel production, approximately 25 cents thereof go to the production of the necessary enzymes [22].

Cellulose, hemicellulose and lignin are the main components of lignocellulosic biomass. But while cellulose consists only of  $\beta$ 1 $\rightarrow$ 4 linked glucose, hemicellulose is a complex heteropolymer containing several types of monosaccharides and is cross-linked to cellulose by lignin, a phenolic polymer. The disintegration and utilization of these components therefore is even more challenging and influences the activity of enzymes used in cellulose depolymerization heavily [11].

Native cellulose contains amorphous regions and recalcitrant crystalline parts which are highly resistant to enzymatic attack. Literature describes two co-active systems of enzymatic depolymerization, the long-known hydrolytic and in parallel the oxidoreductive cellulose degrading system [11], see Figure 2.2.

The hydrolytic mechanism is based on hydrolases and  $\beta$ -glucosidase. Endo-acting hydrolases randomly introduce breaks in the parallel cellulose chains (amorphous regions), while exo-acting hydrolases like cellobiohydrolases chip away  $\beta$ -linked glucose residues of varying length (cellooligosaccharides) from the resulting chain end. Finally  $\beta$ -glucosidases break down the soluble cellooligosaccharides and cellobiose ( $\beta$ 1 $\rightarrow$ 4 linked glucose dimer) into single glucose molecules [11].

The recently discovered oxidoreductive cellulose degrading system helps to overcome the recalcitrance of the highly compact crystalline cellulose regions. Lytic polysaccharide monooxygenases (LPMOs) catalyze an oxidative reaction in exactly these crystalline

environments. The resulting chain breaks, disrupt the cellulose structure, which increases its accessibility to hydrolytic enzymes [13].

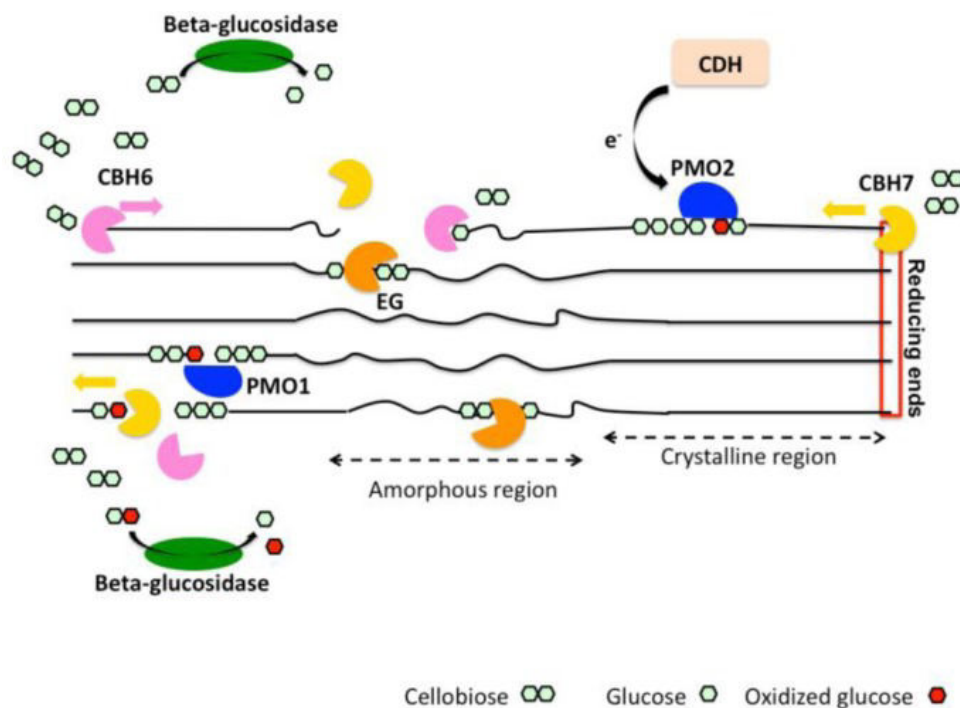


**Figure 2.2.** Schema showing the enzymes necessary for cellulose degradation: cellobiohydrolases (CBH), endoglucanases (EG), lytic polysaccharide mono-oxygenases (PMOs), cellobiose dehydrogenase (CDH) and  $\beta$ -glucosidase [11]

### 2.2.1 Regulation of lignocellulolytic enzyme expression

Filamentous fungi are able to produce and secrete diverse lignocellulolytic enzymes to utilize available lignocellulose in their natural habitat. Depending on the type of plant cell polysaccharide available, this system has to be accurately adapted and fine tuned to break down the complex carbohydrates into fermentable sugars [26]. Gene regulatory proteins (or transcription factors) adjust gene expression by turning distinct sets of genes on or off by binding to a specific DNA sequence, which can be determined experimentally [3]. Understanding these complex regulatory networks on a systemic level helps researchers to rationally engineer the strain through metabolic engineering e.g. overexpressing specific gene expression activators or deleting some repressors and improve enzyme production e.g. by optimizing process conditions [26].

### Targeting transcription factors

Research shows that it is more productive to selectively engineer transcription factors to upregulate expression of enzymes rather than simply overexpressing individual enzyme genes [26]. Li et al. (2015) identified the following major regulators of lignocellulolytic enzymes in the filamentous fungus *Penicillium oxalicum*:

- **ClrB**: key transcription factor which strongly upregulates cellulolytic gene expression (mainly cellulases and some hemicellulases), its deletion seems to lead to reduced cellulase activity, homologs can be found in many fungal proteomes [26]
- **XlnR**: highly conserved regulator with varying functions dependent on the organism, commonly activated transcription of cellulases and/or hemicellulases, in *P. oxalicum* its deletion completely abolished the expression of a major xylanase [26, 37], see fig. ??
- **CreA**: common master regulator in filamentous fungi allowing the utilization of a preferred carbon source while suppressing the consumption of complex polysaccharides by downregulating cellulolytic and xylanolytic gene expression, responding to the carbon in its environment in *P. oxalicum* it tightly regulates the expression of *clrB*, *clrB-2*, *xnlR* and *amyR*, supposedly by a cascade regulation which represses the activator genes of the above mentioned as well as structural genes that potentially are upregulated by those. CreA also seems to be involved in developmental programs like conidia formation and hyphal morphology as well [26].
- **AmyR**: probably controls the balancing between cellulose and starch utilization, a knockout in *P. oxalicum* lead to a dramatically reduced expression of amylase genes but increase cellulase expression [26]

Gene expression is highly regulated and many more gene regulatory proteins are expected to play a role but the listed ones seem to be a promising starting point for the much less investigated *T. aurantiacus*, especially as homologs of all these genes have been described in its genome by Schuerg et al. (2017). Previous studies in closely related organisms like *P. oxalicum* impressively demonstrated that by e.g. deleting *bgl2* (an important intracellular beta-glucosidase) and *creA* together with the over-expression of *clrB* significantly increased the mutants cellulolytic ability as well as the extracellular protein concentration up to 20-fold [51].



## 2.3 Fungi as expression systems

Filamentous fungi have versatile metabolisms, which enables them to degrade a wide variety of organic material. They play a key role in ecosystems by recycling biomass. Therefore they are a major source for industrially produced enzymes like cellulases to depolymerize cellulose for biofuel production, lipases and proteases used in detergents, amylases for starch hydrolysis, or pectinases used in fruit juice production [33].

Due to the high secretion capacity (for cellulases beyond 100 g/L) fungi are the preferred cell factory for many commercially produced enzymes. However, engineering and genetic manipulation of fungi is much more complex than it is for many bacteria and yeasts [48].

### 2.3.1 *Thermoascus aurantiacus*

The thermophilic filamentous fungus *Thermoascus aurantiacus* (TA) belongs to the order of Eurotiales and was first isolated in 1907 from self-heating hay. Its name is derived from the greek *thermos* (hot) and *askos* (tube), as well as the latin *aurantiacus* (orange-colored), due to its brightly orange fruiting bodies (see Fig. 2.3). Like most ascomycota TA forms exceptionally small ascospores for sexual reproduction [39].

Remarkably TA does not only secrete high titers of enzymes, but they are also very active and immensely thermostable and retain their activity at 60 °C for prolonged times [28, 40]. Interestingly the cellulase expression profile is astonishingly simple, consisting only of five major cellulolytic enzymes [39]. These features make TA an interesting host for thermostable cellulase and hemicellulase production.

### Sexual Crossing

Many fungi propagate asexually (anamorphs) [44], but sexual propagation enables organisms (telomorphs) to generate better adapted progeny and to purge harmful mutations [31]. These advantages of sexual reproduction outweigh its disadvantages like the cost of time and energy to recognize and/or attract a mating partner or the risk of transmitting parasites [45].

A main dichotomy in the sexual reproduction of fungi is the distinction between the homothallic and the heterothallic model [31]. Homothallic fungi lack any discrimination at syngamy, meaning that any two vegetative haploid nuclei, even from the same progenitor, can fuse [7]. This fusion between two identical haploid nuclei instantly leads to genome-wide homozygosity (haploid selfing), whereas syngamy with two genetically different vegetative nuclei results in so called outcrossing [45].

Sexual crossing is widely used in research as well as a tool for efficient and quick industrial strain improvement [44]. In the homothallic fungus *T. aurantiacus* sexual crossing can be used to screen progeny for hyper-production strains or to remove disadvantageous mutations [39].

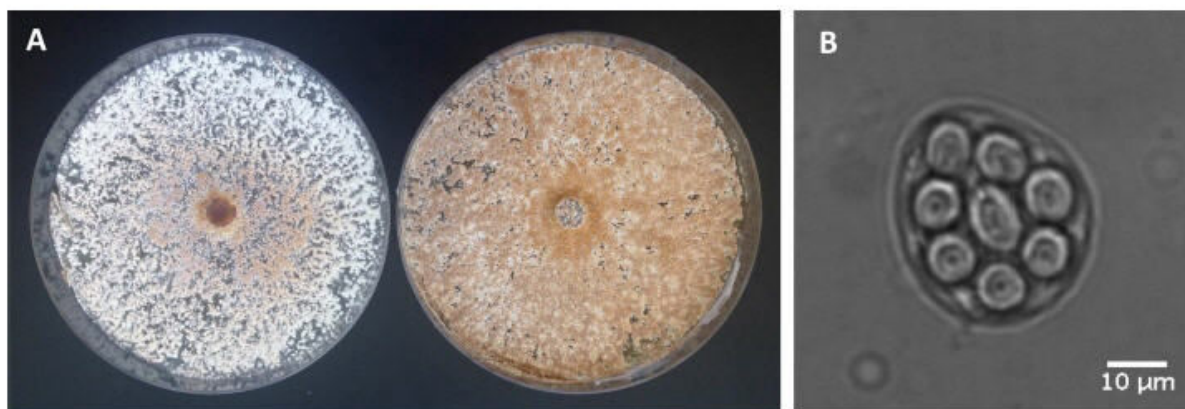


**Figure 2.3.** A. The bright orange fruiting bodies of *T. aurantiacus* after an incubation of 4 days (left) and 11 days (right) on PDA plates

B. Typical ascus of *T. aurantiacus* containing eight ascospores (image from [39])

### Transformation with *Agrobacterium*

*Agrobacterium*-mediated transformation (AMT) is the method of choice for fungal transformation, in organisms like TA where protoplast-mediated transformation (PMT) is not possible. In comparison to PMT, AMT is more labor intensive, but depending on the organisms, also yields high transformation efficiencies [21].

*Agrobacterium tumefaciens* is a gram-negative bacterium and well known plant pathogen causing tumor formation at the site of infection (crown gall disease) [30]. These tumors are caused by the *Agrobacterium* transferring some of its plasmid DNA (T-DNA) leading to uncontrolled growth. Apart from these oncogenes the large tumor inducing plasmid (Ti plasmid) also carries a set of virulence genes, responsible for the actual DNA transfer [16]. As the virulence genes act *in trans* on the T-DNA surrounded by a 24 bp so called border repeat, most commercially available *Agrobacterium* strains are designed to contain a binary vector system (see Fig. 2.4). Therefore the T-DNA was removed from the Ti plasmid, which then acts as a sole helper plasmid to transfer the desired gene of interest between the border repeats from a separately introduced cloning plasmid [21].

After decades of using *A. tumefaciens* as a vector to genetically engineer plants, in the early 2000s researchers demonstrated its effectiveness for fungi and yeast as well [21]. Critical factors that

are influencing AMT efficiency in fungi include the type of fungal starting material (protoplasts, spores, mycelium or fruiting body), the used strains of *Agrobacterium* and hosts and the applied co-cultivation conditions (temperature, pH, various filters) [30]. The virulence genes on the helper plasmid are activated at low pH (5-6) and when the *Agrobacterium* senses a phenolic inducer like acetosyringone, imitating substances released by wounded plant cells [21]. A phosphorylation cascade ultimately leads to the release and translocation of a single stranded copy of the T-DNA into the infected cell (see Fig. 2.4) [21].

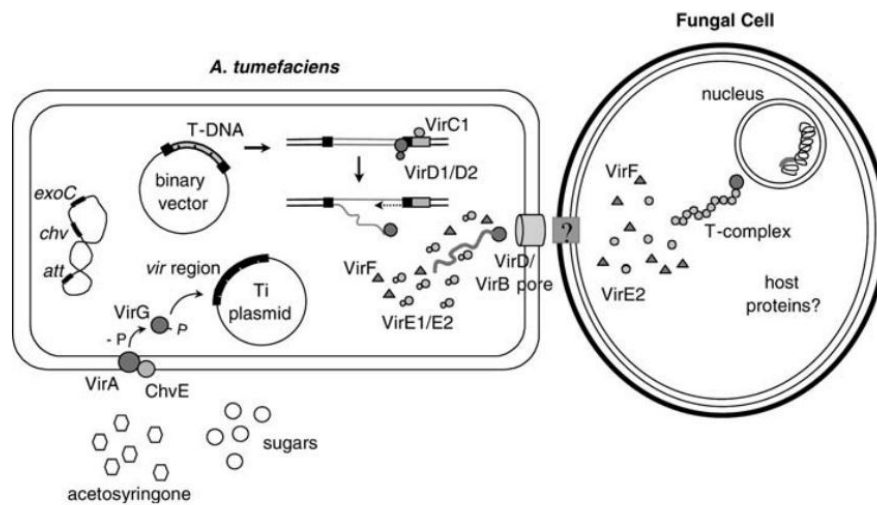


**Figure 2.4.** Schema of the *Agrobacterium* mediated T-DNA transfer system [30].

### Selection systems

To screen for successful transformants or mutants in general researchers rely on selection markers. Dominant selection makers provide the host with a new function, e.g. the resistance to a specific antibiotic. Auxotrophic selection on the other hand requires an auxotrophic strain, carrying a mutation limiting its growth due to the inability to synthesize a particular compound - auxotrophic markers can therefore restore normal growth in these mutants [47].

To generate strains with several mutations (stacking), the number of available selection makers is often limiting as once a selection mechanism is applied it cannot be used to screen for any subsequent editing steps. Recyclable markers which are removed from the genome after the selection are a good alternative. This system was first demonstrated in 1987 by Alani et al. in *Saccharomyces cerevisiae* with *URA3* [2, 47]. Orotidine-5'-phosphate decarboxylase is a key enzyme in the pyrimidine biosynthesis and strains with a disrupted *URA3* therefore require the pyrimidine derivative uracil in the media. As an auxotrophic selection marker *URA3*

deficient strains can be counter-selected with 5-fluoroorotic acid (5-FOA) as an active Orotidine-5'-phosphate decarboxylase will metabolize 5-FOA into the lethal 5-fluorouracil [47].

This selection maker can be re-used after the deficient *URA3* is restored by mitotic recombination with a construct containing flanking direct repeats [47] (see Fig. 2.5).

In TA the targets to create such a recyclable marker system are *pyrE* and *pyrG* (*S. cerevisiae* *URA3* orthologues) causing uracil auxotrophy and 5-FOA resistance, as well as *amdS*.

The acetamidase gene *amdS* is commonly used as a "gain of function" selection marker in other fungi, but occurs naturally in TA. With a functional enzyme the organism is able to grow on acetamide as sole carbon or nitrogen source by hydrolyzing it to acetate and ammonia [47]. Like the *ura5* orthologues, *amdS* can be recycled and counter-selected on media containing fluoroacetamide (FAA), which is metabolized by an active acetamidase to the cell-toxic fluoroacetate [47] (see Fig. 2.5). Unlike a *pyrE/pyrG* deficiency, an *amdS* mutation does not lead to any growth defect on regular media.

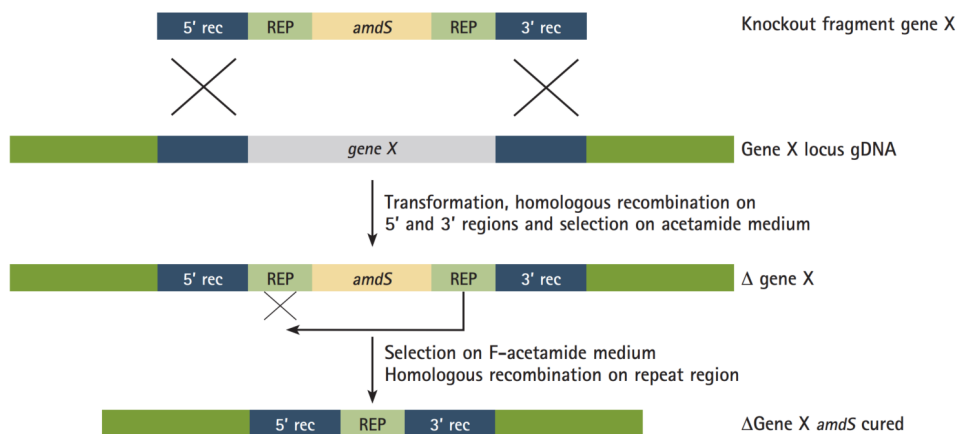


**Figure 2.5.** Schema of a targeted gene knockout and selection on FAA, utilizing *amdS* as a recyclable marker [49]. The construct contains 5' and 3' flanking regions (blue) for homologous recombination. Subsequently the knockout strain loses the *amdS* through selection on FAA by homologous recombination of the repeat sequences (light green) on both sides [49].

A similar selection approach was chosen to select for potential *creA* mutants. The toxic sugar analog 2-deoxy-D-glucose (DOG) is phosphorylated by the fungal hexokinase and the resulting compound (2-deoxyglucose-6-phosphate) blocks any further steps in glycolysis [4].

Because *creA* is regulating the uptake of the preferred carbon source, knockout strains seem

to be more resistant as they more readily metabolize other complex sugars. Thus, DOG is often used to identify fungal mutants that are not able to repress secretion of cellulases and hemicellulases in the presence of easy available carbon sources, which is a beneficial phenotype for producing high amounts of enzymes.

## 2.4 Genetic Manipulation of microbial strains

### 2.4.1 Directed Mutagenesis

Ever since the discovery of the DNA double helix as the molecule that ultimately enables all life on earth, researchers have been searching for technology to manipulate its code. Over the last 60 years of biological research several methods to selectively edit the genetic code have been developed, deployed and refined. Still the hunt for a reliable and easy-to-use targeted genome editing tool continued until the unstoppable rise of CRISPR-Cas9 five years ago [12].

#### CRISPR-Cas9

Since the mid-2000s several research groups started to look into clustered regularly interspaced short palindromic repeats (CRISPR) that were first described by a Japanese team in 1987 in *E. coli*. The CRISPR-Cas (CRISPR-related nuclease) system is an adaptive defense system found in many bacteria, that uses DNA fragments of the intruders which are then integrated in a specific part of the hosts genome - the CRISPR array - where they are interspaced with short sequences. These bits are then transcribed as pre-crRNA (CRISPR RNA) and mature to single individual crRNAs composed of the short intermediate sequence by the host and the part of invasive DNA. The crRNA then serves as a guide for the Cas nucleases to site specifically cleave foreign nucleic acids [12].

So far, three different CRISPR-Cas9 systems have been identified in bacteria, but only the type II requires a single Cas protein, which showed to be extremely useful for genome engineering. This large Cas9 protein contains two nuclease domains (HNH and RuvC-like) and requires a second small RNA that is encoded further upstream and supports the maturation of the crRNA. The fusion of this trans-activating crRNA (tracrRNA) and the actual crRNA lead to the development of the CRISPR-Cas9 system as it is used today - a simple system consisting only of two components: the single guide RNA (sgRNA) and the Cas9 nuclease. This sgRNA now contains a 20-nucleotide long sequence at the 5'end (protospacer) recognizing specifically the targeted DNA sequence by Watson-Crick base pairing, and the sequence at the 3' end binding the respective Cas9 protein. The only restriction when targeting any DNA sequence is

the presence of a 2-6 bp protospacer adjacent motive (PAM), a Cas protein specific sequence motive close to the binding site of the sgRNA where the nuclease ultimately introduces a double strand break [12].

Upon a double strand break in genomic DNA (gDNA), it is repaired either by non-homologous end-joining (NHEJ) leading to random loss, insertion or replacement of bases or homologous repairing (HR) where entire exogenous DNA fragments are inserted at the point of breakage. Approximately half of the mutations induced by CRISPR-Cas9 were shown to be at single base insertions (mainly A or T), followed by relatively small deletions (between 1-50 bp) and rarely base substitutions of two or more basepairs [48].

For eukaryotic organisms with their much more complex genomic background, making genetic engineering more challenging, CRISPR-Cas9 has revolutionized research [48]. Nodvig et al. (2015) were one of the first teams to create an efficient CRISPR-Cas9 system for filamentous fungi. Therefore both components had to be modified:

- **Cas9:** to enhance functionality the *cas9* gene originating from *Streptococcus pyogenes* was codon-optimized and the classic nuclear localization signal of simian virus 40 (SV40) was added on the 3'end to ensure transportation of the protein to the nucleus [33]. A constitutive promoter is used to ensure successful expression, like in our CRISPR-Cas9 system the RNA polymerase II promoter *tef1*, see Fig. 7.4.
- **sgRNA:** to avoid the attachment of a 5' cap and 3' poly A-tail, the sgRNA is flanked by two self-cleaving ribozymes, the hammerhead (HH) ribozyme on the 5'end and on the 3' end the hepatitis delta virus (HDV), see Fig. 2.6. This construct simultaneously allows to concatenate the gRNAs and target several genes at the same time - a technique called multiplexing [48].

To guarantee robust synthesis of the sgRNA it is preceded by a strong constitutive promoter like *gpdA* from *A. nidulans* and typically followed by the *trpC* terminator, see Fig. 7.4 [33, 32].

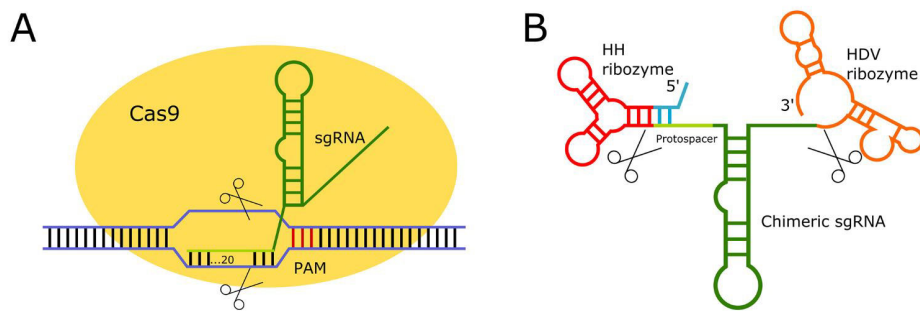


**Figure 2.6.** **A.** Schema of the CRISPR-Cas9 system with the sgRNA binding to Cas9 and base pairing the target DNA behind the PAM sequence.

**B.** The sgRNA embedded between the self-cleaving ribozymes [33].

### 2.4.2 Random mutagenesis

Before research had tools at hand to targeted manipulate the genetic code, most genes were identified by the abnormalities their mutation produced. To quickly generate large numbers of mutants whose genetic code deviates from the wt, DNA damaging chemicals or radiations are commonly used. Random mutagenesis can lead to surprising discoveries, but requires extensive screening [3].

## 2.5 Relevance

With the upcoming shortage of fossil fuels and the associated disastrous environmental problems they are causing, the need for a renewable, cheap and versatile alternative fuel resource becomes urgent. Biofuels, especially second generation biofuels from non edible biomass, have been an interesting option for decades. The limiting step thereby often is the depolymerization of cellulose to its glucose components.

Several well performing enzyme mixtures therefore are already commercially available, that unfortunately are quite temperature sensitive and require a lot of cooling, which dramatically increases process costs. The thermophilic ascomycete fungus *Thermoascus aurantiacus* (TA) is an intriguing host for the production of cellulolytic enzymes as it is naturally secreting high titers of thermostable enzymes. While genetic engineering tools such as the CRISPR/Cas9 system have been recently developed for this fungus, virtually nothing is known about the genetic regulation of thermostable enzymes, which is necessary for performing strain engineering efforts to increase enzyme production for cost-efficient biofuel generation.

## 2.6 Strategy and Objective

To gain a deeper understanding of the complex regulatory network controlling the production of cellulolytic enzymes in *T. aurantiacus* we chose several different approaches to enhance our knowledge from various angles.

By targeting specific genes that are known in other fungi to regulate cellulase secretion, a reliable system for site-directed mutagenesis is required. By further employing the prior developed protocols for *Agrobacterium* mediated transformation and the CRISPR-Cas9 system we hoped to make working with *T. aurantiacus* more predictable. From the desired gene knockouts we intended to expand out knowledge on the regulation of cellulolytic enzyme expression in TA.

Random mutagenesis and sexual crossing experiments were additionally used to quickly generate larger numbers of mutants, which we can then screen for desired traits e.g. carbon catabolite derepression or auxotrophies that can be further used for strain engineering efforts.



---

## 3 Material and Methods

### 3.1 Microbiology methods

#### 3.1.1 Cultivation conditions, media and strains

The wild type (wt) *Thermoascus aurantiacus* (American Type Cell Culture Collection No. 26904) was provided by the laboratory as a -80 °C cryo-stock. It can be inoculated directly from the cryo-culture or by transferring a piece of overgrown agar on potato dextrose agar (PDA) plates. Alternatively *T. aurantiacus* can be cultivated on minimal media agar plates with 1-2 % carbon source and Vogel's Medium N salts [29]. These are then incubated for 2 days at 50 °C and further 4 days on 45 °C in a humid atmosphere to avoid desiccation.

For the liquid culture experiments we used a slightly modified form of McClendon's media [28]. Therefore component I, an organic nitrogen source (component II: soy peptone 0.8 % w/v) and a carbon source (component III: e.g. avicel, xylan etc. 2 % w/v) are mixed and autoclaved. 50 mL of the prepared media were inoculated with  $10^6$  spores and incubated in a baffled 250 mL shake flask at 50 °C for 3 days at 180 rpm.

Experiments to scale down the liquid media experiments to cultivate several mutants in a single plate (e.g. in a FlowerPlate in BioLector with a volume up to 1000  $\mu$ L or in a 24-well plate with 300-500  $\mu$ L, covered with AeraSeal sealing film by Excel Scientific) failed. The high optimal growth temperature, as well as for filamentous fungi typical pellet formation lead to high evaporation and extremely low protein secretion titers.

#### 3.1.2 Preparation of competent cells

##### **Electrocompetent *Agrobacterium tumefaciens***

*Agrobacterium tumefaciens* is made electrocompetent to transform the cells with plasmid DNA by electroporation.

A -80 °C stock of *A. tumefaciens* strain APA 4600 (EHA 105) is cultivated on LB agar plates for 2 days at 30 °C. The cells are further grown in liquid culture (100 mL LB broth) overnight at 30°C on a 250 rpm shaker. Thereof 1 mL are transferred to 100 mL fresh LB broth and grown to an OD<sub>600</sub> of 1.

The culture is centrifuged at 4000 rpm for 15 minutes at 4 °C. The resulting pellet is resuspended in 25 mL 1 mM icecold HEPES buffer (pH 7.0). The suspension is centrifuged again at the same

conditions and the pellet resuspended in 0.5 mL 1 mM HEPES Buffer (pH 7.0) containing 10 % glycerol. Aliquots of this cell suspension are then frozen at -80 °C in eppendorf tubes.

### 3.1.3 Transformation

#### Transformation of *Agrobacterium* with plasmid DNA by electroporation

The prepared electrocompetent *Agrobacterium tumefaciens* cultures are thawed and 50 µL thereof incubated with 500 ng to 1 µg of plasmid DNA on ice for 2 minutes. The cell-DNA mixture is transferred to a chilled BioRad electroporation cuvette. The capacitor of the electroporator (Gene Pulser Xcell, Biorad) is set to 25 µF and the pulse controller to 400 ohms. A single electrical pulse of 2.5 kV is applied at a field strength of 12.5 kV/cm.

1 mL of LB broth is added to the cuvette and the gently resuspended. The cell suspension is transferred to a fresh tube and incubated at 30 °C at a tilted angle of 45° at 250 rpm for 2 hours. The samples are then plated on LB agar plates containing kanamycin and incubated upside down at 30 °C. After 2 to 3 days the transformed colonies can be picked.

#### *Agrobacterium* mediated transformation of *Thermoascus aurantiacus*

The plant pathogen *Agrobacterium tumefaciens*, which until twenty years ago had only be used to edit the genome of plants, is nowadays commonly used to transform yeasts and fungi [21]. The following protocol for TA transformation has been developed by Raphael Gabriel and Julia Prinz.

PDA plates (Teknova, Hollister, USA) are inoculated with *Thermoascus aurantiacus* cultures and incubated for 2 days at 50 °C followed by an incubation at 45 °C for 4 days in an humid environment.

Meanwhile the *Agrobacterium* carrying the plasmid of interest are streaked out on LB agar plates containing the appropriate antibiotic, in this case kanamycin, and incubated for 3 days at 30 °C. Then an *Agrobacterium* colony can be picked and cultured overnight in 10 mL LB broth with antibiotics at 30 °C on a shaker (200 rpm).

The next morning the OD<sub>600</sub> of the culture is measured and then diluted with LB<sub>kan</sub> media to an OD<sub>600</sub> of 0.5. In this step triplicates are prepared, which are further incubated for approximately 90 minutes until the OD<sub>600</sub> is between 0.85 and 1. The cultures are then transferred to 15 mL falcon tubes and centrifuged at 4000 rpm for 10 min, before the supernatant is carefully discarded. Next 10 mL of liquid induction media, containing the phenolic inducer acetosyringone (4'-Hydroxy-3',5'-dimethoxyacetophenone), is added (see Appendix, 7.3) and the

pellet resuspended. This step is repeated once more before the bacterial cells are cultured for 24 h at 30 °C on a shaker (200 rpm) for induction.

After an incubation of in total 6 days the *Thermoascus* spores are harvested by adding 5 mL of sterile Tween 0.8 % onto the plate and gentle scraping with a spatula. The resulting suspension is centrifuged (4000 rpm, 10 min) and filtered through Miracloth (Milipore Sigma, No. 575855) to remove any remaining cell material. The spore suspension is centrifuged again (4000 rpm, 10 min) and the supernatant reduced to app. 10 ml. The pellet is resuspended and the spores counted with a hemocytometer under the microscope. The suspension is then diluted to contain  $10^8$  spores/mL.

For the actual transformation a vacuum filter system is used to combine 1 mL of the fungal spore solution and 2 mL of the *A. tumefaciens* carrying the plasmid of interest on a filter. It is then transferred to a small agar plate containing 250 µL/mL cefotaxime to kill the *Agrobacteria* and incubated at 28 °C for 48 h.

Finally each membrane is vortexed in a flacon tube with 5 mL of H<sub>2</sub>O containing 250 µL/mL cefotaxime. The resulting spore suspension is spun down (4000 rpm, 10 min) and the pellet resuspended and plated on appropriate selection plates. These are incubated at 45 °C for at least 24 h.

### 3.1.4 Sexual Crossing

Sexual crossing was performed according to a protocol developed by Julia Prinz.

Cultivated TA strains can be crossed on potato dextrose agar plates by placing small agar pieces abundantly covered with fungal mycelium twice on opposite sites of the plate. These are then incubated for 6 days at 45 °C, after which the spores at the interface between the two strains can be harvested, filtered to remove any mycelium and eventually in a dilution spread on appropriate selection media. The selection plates are further incubated at 45 °C for 2 days until single colonies can be picked and subcultured on PDA medium containing possibly required supplements.

Crossed strains were cryo-conserved and verified by Sanger sequencing of the gene of interest.

## 3.2 Molecular biology methods

### 3.2.1 Genomic DNA extraction

Extraction of genomic DNA from *T. aurantiacus* was performed according to a protocol developed by Julia Prinz and Carlos Romero.

After the required cultivation on solid media, some the fungal body (mycelium and spores) is scaped off the plate with a disposable scraper and by adding 5 mL dH<sub>2</sub>O. The collected suspension is spun down and the supernatant removed. The pellet is transferred to a 2 mL microtube containing 0.5 mm Zirconia/Silica beads and a single big 5.0 mm Ytria bead. Then 500 µL of Tail Lysis Buffer as well as 10 µL of RNase A (both from the Maxwell kit) added.

The tubes are put in the FastPrep-24 5G bead-beater (MP Biomedicals, Irvine, CA, USA) and run for 30 sec on the Fungal setting. Next the tubes are centrifuged at maximal rpm for 5 min to remove any solid particles from the sample lysate. This supernatant is then processed in the Maxwell RSC Instrument (Promega, Madison, Wisconsin, USA) according to the protocol for plant DNA.

### 3.2.2 Amplification of DNA

To amplify DNA, first primers were designed with the Geneious Prime Software (Biomatters Ltd., Auckland, New Zealand) and ordered at IDT (Integrated DNA Technologies Inc., San Jose, USA). For the Polymerase Chain Reaction (PCR) we used the Q5 Hot Start High-Fidelity DNA Polymerase (Cat. No. M0493, New England BioLabs, Ipswich, Massachusetts, USA) or One Taq Quick-Load 2X Master Mix (Cat. No. M0486S, NEB) and followed the respective protocol. The annealing temperature for the specific primers was calculated with the NEB T<sub>m</sub> calculator (see <https://tmcalculator.neb.com>).

Amplified DNA fragments can directly be isolated with the PCR purification kit (QIAquick PCR Purification Kit, QIAGEN).

### 3.2.3 Gel electrophoresis

To check or purify PCR products, depending on the expected product size, a 1 % or 1.5 % agarose gel with GelRed was used. 1X Tris-acetate-EDTA (TAE) buffer, diluted from TAE 50X (Teknova, Hollister, CA, USA), was used to prepare the gel and running it. Typically the gel electrophoresis was run at 120 V for 30 minutes with a Power Supply Station (PowerPac, Biorad).

Gel extraction was performed with the QUIAEX II Gel Extraction Kit (150) (Cat. No. 20021, QIAGEN, Hilden, Germany) according to the given protocol.

Nucleic acid concentration was measured with the NanoDrop 2000 (Thermo Fisher Scientific, Waltham, Massachusetts, USA) at 260 nm and the purity estimated from the 260/280 nm ratio.

### 3.2.4 Mutagenesis

To develop new mutants with desired traits like a new selection system or impaired catabolite repression from the *Thermoascus aurantiacus* wt we tried chemical random mutagenesis with Ethyl methanesulfonate (EMS) and mutagenesis by radiation using ultraviolet light (UV).

For the chemical mutagenesis, a spore suspension of  $1 \cdot 10^7$  spores/mL was combined with 10 % v/v EMS and shaken incubated for a defined amount of times, ranging between 15 to 60 minutes. The resulting spores were incubated for 3 days at 45 °C on appropriate selection plates.

The mutagenesis by radiation was performed on 15 mL of a spore suspension with  $5 \cdot 10^7$  spores/mL, that was exposed to UV light for 20 or 40 seconds in the UV Crosslinker (FB-UVXÖL-1000, Fisher Scientific).

### 3.2.5 Cloning

#### Plasmid Design

Using the basic design of the CRISPR/Cas9 Knockout plasmid for TA provided by Julia Prinz (see Figure 7.4), only the 20 bp protospacer and the 6 bp reverse complement sequence were exchanged according to the targeted gene of interest to be knocked out. The protospacer sequence was generated with the online tool CRISPOR [17], see <http://crispor.tefor.net/>, for *Thermoascus aurantiacus* with the 20bp-NGG - Sp Cas9 Protospacer Adjacent Motif (PAM).

This CRISPR/Cas9 knockout plasmid used to be assembled with Gibson, however a different approach was chosen in this project as the length of the insert containing the specific gRNA sequence is relatively small compared to the massive (12kb) backbone. This new approach allows for a more reliable and less error-prone plasmid assembly and cloning and, was developed in collaboration with Henrique De Paoli and the DIVA Team (see Figure 3.1).

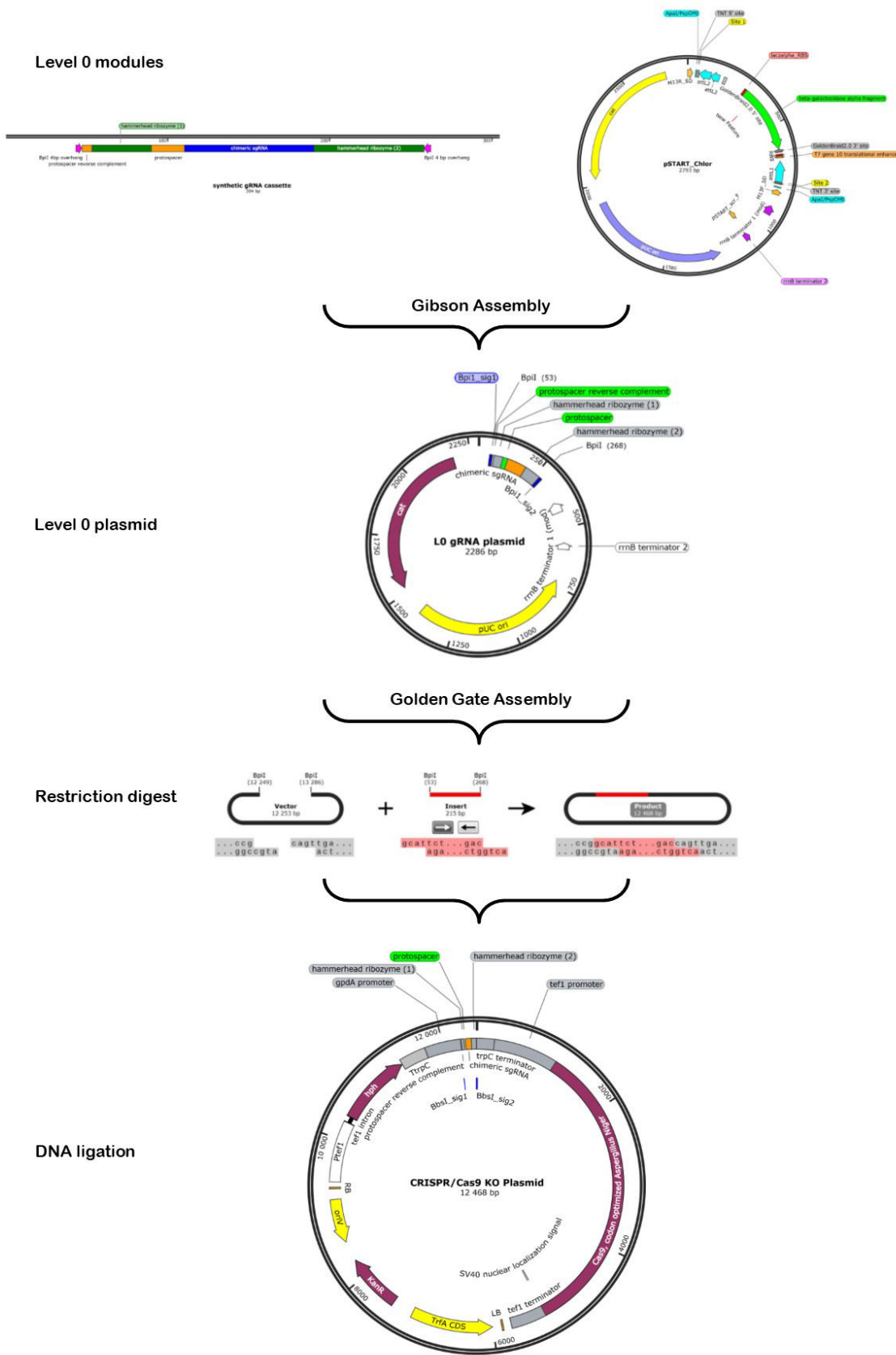


Figure 3.1. Schema of the cloning strategy (created with the SnapGene Software [42]).

The original CRISPR/Cas9 plasmid is based on the pTS57 plasmid developed by Simon Harth for a high throughput cloning system and constitutive gene expression.

The 211 bp long gRNA cassette was first cloned into a pSTART\_Chlor vector (created by Nathan Hillson at JBEI, see [36]) carrying a Chloramphenicol resistance (see Figure 7.1), which can easily be accomplished by a Gibson assembly and called Level Zero gRNA plasmid (L0 gRNA). The gRNA part (304 bp) was synthesized as a gBlock Gene Fragment by IDT.

The actual knockout plasmid backbone carrying the Cas9 gene on the other hand was modified to carry a drop-out GFP cassette for easy Green-White screening (see Figure 7.3) and likewise assembled with Gibson. To select for successful TA transformants the plasmids contains a hygromycin B phosphotransferase resistance marker (*hph*) flanked by the native translation elongation factor-1 (*Ptef-1*) and the tryptophan biosynthesis protein terminator (*trpC*).

The GFP cassette as well as the gRNA part in the L0 plasmid are enclosed by recognition sites for the Type II restriction enzyme BpiI (isoschizomer: BbsI), generating a specific 4 bp overhang (see Figure 7.2) which can be utilized for Golden Gate Cloning.

Plasmids were designed with the Geneious Prime Software and uploaded to JBEI's DIVA (Design, Implementation, and Validation Automation) Service, a web-based software platform enabling researchers to design and submit DNA constructs to internal resources for construction. Via the DIVA website, the designed plasmid is linked to the internal Inventory of Composable Elements (ICE), where each strain and plasmid is archived and available to be ordered. Uploaded plasmid designs are then run with the j5 DNA Assembly Design Automation Software, which automatically designs cost-optimal and scar-less multipart DNA assembly protocols [20]. The user selects the method of choice for DNA assembly, like Gibson or Golden Gate, defines the DNA parts that are to be assembled and may manipulate a set of user-adjustable parameters e.g. the maximum length of oligos to be synthesized.

### **Gibson Assembly**

PCR fragments were provided by the DIVA Team and synthetic parts ordered as gBlocks at IDT and first assembled by Gibson, using the ECHO 550 Liquid Handler (Labcyte, San Jose, CA, USA) with the Gibson Assembly Cloning Kit (Cat. No. E5510S, NEB) according to the manual. Plasmids were transformed into commercially available competent *E. coli*, like NEB 5-alpha (NEB), and further incubated on LB medium containing appropriate antibiotics.

Assembled L0 gRNA plasmids were verified with a restriction digest and Sanger sequencing at Genewiz. Successfully assembled BpiI KO plasmid can be distinguished by a restriction digest

as well as Green-White screening, as upon successful assembly they should express GFP as well.

### Golden Gate Cloning

The Mastermix prepared for Golden Gate Cloning contained 80 U of T4 DNA Ligase (Thermo Fisher Scientific), 2.5 U of the restriction enzyme BbsI-HF (NEB) and CutSmart Buffer (NEB) supplemented with 1 mM ATP. We used 75 ng of vector backbone (Bpi1 KO plasmid) and an equimolar amount of insert (L0 gRNA plasmids). Total reaction volume was 10  $\mu$ L, which was obtained with nuclease free water.

The mixture was incubated in a thermocycler at 37 °C for 2 minutes, followed by 5 minutes at 16 °C - for 50 cycles. Thereof we used 1  $\mu$ L to transform chemically competent *E. coli*.

Colonies carrying the properly assembled plasmid was identified with Green-White-Screening, as the GFP insert is exchanged with the gRNA cassette (a complete list all plasmids can be found at Tab. 7.2).

### 3.2.6 Purification of plasmid DNA

To purify plasmid DNA, the QIAprep Spin Miniprep Kit 250 (QUIAGEN) was used according to the respective protocol.

### 3.2.7 DNA Sequencing

#### Plasmids

To verify the generated plasmids, they were sequenced with the in-house DIVA sequencing service. It uses the high throughput Next Generation Sequencing (NGS) MiSeq system by Illumina, which has the advantages of a relatively low error rate and high coverage.

Library preparation is conducted with the Nextera XT DNA Library Preparation Kit (Illumina). Submitted samples are first fragmented, followed by a tagmentation step with universal Illumina adapters and amplification. Fragments are then pooled according to the most abundant fragment size (app. 350 bp) and purified before actually being sequenced.

Results are aligned to the respective ICE entry and automatically analyzed by read-mapping using the BWA-MEM algorithm [25] and variant-calling with the GATK HaplotypeCaller software [6]. The alignment files as well as a quality control (QC) report containing the percentage completed, coverage and variants were provided.



**PCR amplicons**

To check for mutations in genes of interests, these were PCR amplified, purified and sent to Genewiz (South San Francisco, CA, USA) for Sanger Sequencing.

## 4 Results and Analysis

### 4.1 Random mutagenesis of *T. aurantiacus* wild type

To generate novel recyclable selection systems and to obtain potential carbon catabolite derepressed TA strains, we tried to mutate the wt with EMS and UV radiation.

After some initial trials to determine the appropriate UV exposure time and EMS concentration to balance the generation of enough mutants while not killing all the cells, the mutated TA spores were spread on plates containing appropriate selection substances.

Selection on 5-FOA plates that helped to isolate *pyrE* or *pyrG* deletion strains resulted in no colonies, whereas on FAA (targeting *amdS*) and DOG (*creA*) selection media, growth was observed on the plate. The mechanisms behind these selection systems were described in section 2.3.1. Deletion of *pyrE* or *pyrG* causes uracil auxotrophy and resistance 5-FOA, which is metabolized to a lethal component in the wt. FAA is similarly toxic for TA if the acetamidase gene *amdS* is active. We can use DOG to select for carbon catabolite derepressed strains, as in the wt it is readily metabolized and blocks further steps in the glycolysis.

The strains growing on the latter media were then isolated and subcultured on minimal media with a higher concentration of the selection substance to remove background spores from the initial plate. Only mutants thereby still growing significantly stronger in comparison to the wt were further cultivated and the respective gene of interest (*amdS*, *creA*) amplified and sequenced. Notably several other mutations in genes other than *creA* can cause a carbon catabolite derepression.

The strains selected on DOG and sequenced exhibited several mutations within the *creA* gene (see Fig. 4.1). Most of those however did not grow well after further cultivation. Therefore we decided to end the attempts to randomly generate a mutation within this gene and focused on recombinant methods. However, it certainly would have been interesting to compare the production of cellulases to the wt, and to further test these strains on different DOG concentrations.



**Figure 4.1.** Sequencing results of three selected putative carbon catabolite derepressed strains isolated from EMS random mutagenesis showing mutations in the *creA* gene, mapped to the wt reference (in green at the top).

Generated with Geneious Prime [1].

All strains selected on FAA showed several mutations in the *amdS* gene (see Fig. 4.2). We concluded that the impaired *amdS* indeed caused a resistance to FAA, as was expected. Most of these strains however exhibited a heavily distorted phenotype e.g. an unusual thick white aerial mycelium (see 4.5). We further tried to cross some of the less aberrant strains with the wt to potentially get rid of excessive mutations and the often extremely distorted phenotype (see chapter 4.2.2).

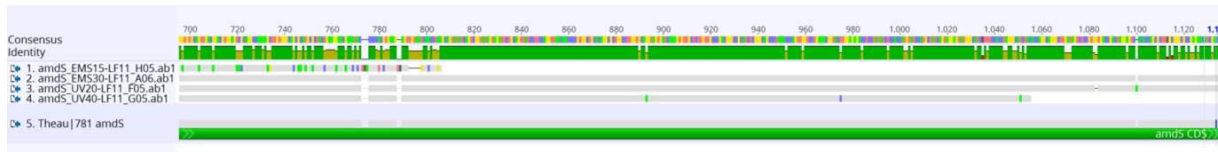


**Figure 4.2.** Sequencing results of four strains selected on FAA after UV or EMS random mutagenesis, mapped to the reference *amdS* gene (in green at the bottom).

Generated with Geneious Prime [1].

In summary, several strains with mutations in the *amdS* gene were isolated from FAA plates and several CCR deficient strains, displaying growth defects, were generated from which few contained mutations in *creA*.

## 4.2 Sexual crossing results

We developed a sexual crossing protocol for TA, to combine desired mutations present in separate strains or remove disadvantageous mutations from one mutant strains by back-crossing with the wt strain.

### 4.2.1 Crossing of $\Delta ku70$ and 5-FOA resistant strain (45-3)

As described in section 2.3.1, a uracil auxotrophic and therefore 5-FOA resistant strain can be used as a selectable marker to overexpress or delete genes of interest. Raphael Gabriel generated

such a TA strain by UV mutagenesis and subsequent selection on 5-FOA. The so called 45-3 has mutations in *pyrE*.

Ku70 is an indispensable protein in the non-homologous end joining (NHEJ) mechanism once a DNA double strand break occurs. Strains with a deficient *ku70* gene are prone to a much higher mutation rate [35]. This is based on the substantially higher homologous recombination (HR) rate in DNA repair, which is more error prone.

This strain was generated by collaborators at PNNL by deleting *ku70* through inserting a hygromycin resistance (*hph*).

Our goal was to cross the available TA  $\Delta ku70$  strain with the *pyrE*-impaired 45-3 to develop of a novel recyclable selection system in TA, carrying a uracil auxotrophy for easy selection as well as a high recombination rate to easily remove the marker again.

The 45-3 mutant with the non-functional *pyrE* gene and the hygromycin resistant *ku70* deletion strain were crossed and the progeny was isolated on minimal medium plates containing hygromycin, 5-FOA and uracil. To verify whether the crossed strains actually exhibit the expected resistances and auxotrophies we cultivated them on minimal media with various supplements (see Fig. 4.3).

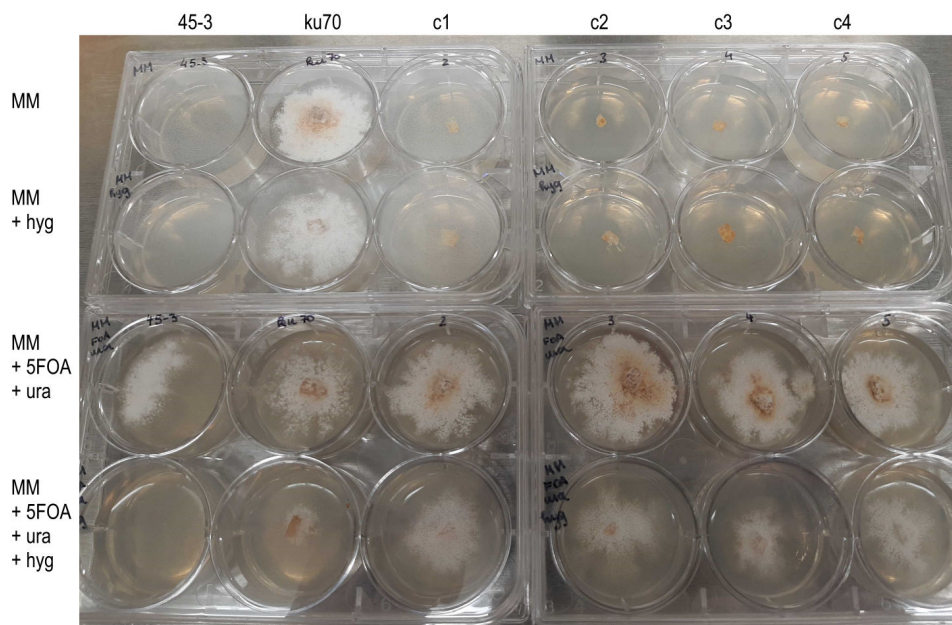


**Figure 4.3.** Verification of the  $\Delta ku70$  x  $\Delta pyrE$  crossing products (c1-c4) by growing them and their source strains on minimal media (MM), minimal media with hygromycin (hyg), minimal media with 5-FOA and uracil (ura) and all of the above combined.

Due to sexual crossing, the  $\Delta ku70$  strain passes a hygromycin resistance to its crossed progeny and because of the knocked out *pyrE* in 45-3 the outcome should be 5-FOA resistant and dependent on supplemented uracil. This double resistance of the crossed progeny was used to isolate the crossed sexual spores in the first place. The resulting crossing products (in Fig. 4.3: c1 to c4) displayed the expected behavior by growing on MM + 5-FOA + ura as well as on MM + 5-FOA + ura + hyg. Equally expected was the outcome for the native 45-3 strain, it only grew on MM + 5-FOA + ura but does not carry a resistance to hygromycin.

Surprising however was the strong growth of the original  $\Delta ku70$  strain on the media containing 5-FOA (see Fig. 4.3), indicating a mutation in its *pyrE* or *pyrG* genes as well. Therefore we sequenced both genes of the original  $\Delta ku70$  cryo stock as well as the two subcultures thereof, that had been used for the crossing and were kept at room temperature on PDA media for a few weeks. All three samples showed two deletions in the *pyrG* gene (see Fig. 4.4) but non in the *pyrE*.

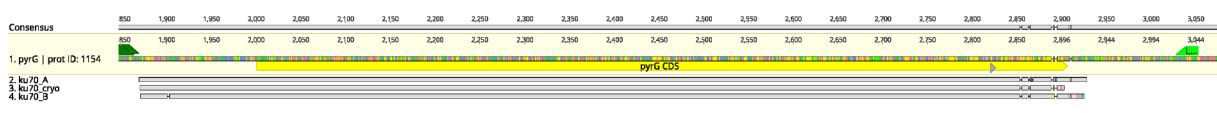


**Figure 4.4.** Sequencing results of the amplified *pyrG* of the original  $\Delta ku70$  cryo stock (cryo) and the sub-cultivates thereof used for crossing (A, B), mapped to the reference *pyrG* (in yellow at the top).

Generated with Geneious Prime [1].

Interestingly one of the  $\Delta ku70$  sub-cultivars from the cryo stock (A) even had a third deletion. This confirms our suspicion that due to the impaired NHEJ pathway this strain is even more prone to genomic instability than expected.

Sequencing of the *pyrE* showed that all crossed progeny inherited the same mutation from 45-3. This uniform mutation in the *pyrE* as well as the inherited hygromycin resistance indicate that the crossing procedure worked reliably. But because of the seemingly high genomic instability of the  $\Delta ku70$ , we have to expect them to carry numerous additional but unknown mutations, making future experiments highly unreliable. Achieving higher deletion efficiency can more safely be obtained by using the CRISPR/Cas9 system.

### 4.2.2 Crossing of $\Delta amdS$ strains from random mutagenesis and wild type

As described above (see section 4.1) we attempted to back-cross some of the  $\Delta amdS$  strains generated with random mutagenesis with the wt, to overcome some of the numerous mutations generated from radiation and chemicals leading to the observed abnormal phenotypes (see Fig. 4.5, A).

This attempt certainly deviated from the regular crossing procedure, as the wt does not convey any selectable marker and we had no way of screening for successfully crossed colonies. The selection only on FAA might lead to a propagation of spores coming only from the  $\Delta amdS$  strains. However, we wanted to see if we could retrieve FAA-resistant strains with a more TA wt typical phenotype.

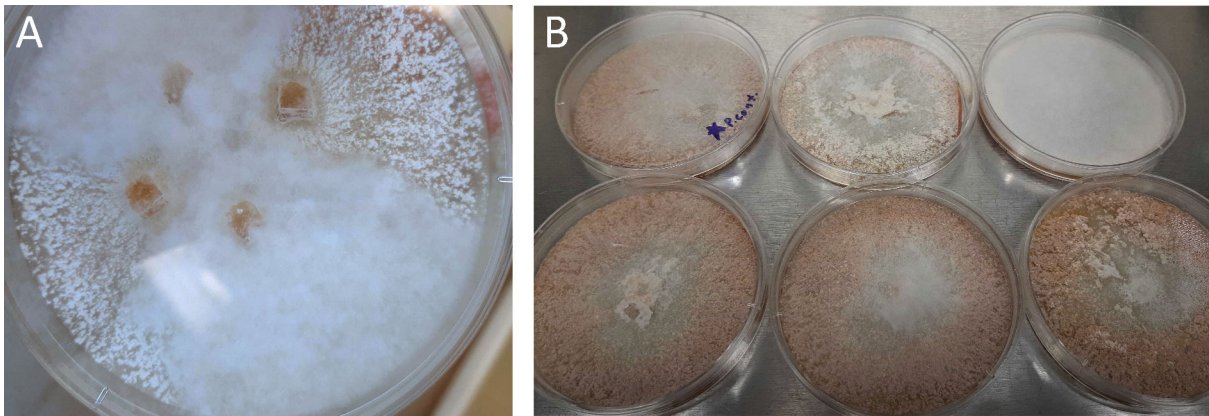


**Figure 4.5.** Crossing of a  $\Delta amdS$  strains generated by random mutagenesis and TA wt

- A.** The  $amdS$  mutant (white aerial mycelium, upper and lower quarter) and the wt (right and left quarter) growing together on a PDA plate (day 4)
- B.** Isolated crossed progeny on MM+FAA exhibiting various phenotypes

For this crossing experiment we choose a FAA-resistant strain with relative low number of mutations within the  $amdS$  gene, but with a peculiar phenotype. Crossed strains were selected according to the closest phenotype resemblance of the wt (see Fig. 4.5, B).

All crossed progeny still carried a FAA resistance but the phenotypes varied heavily, ranging from delicately spun white aerial mycelium covering the entire plate to single patches of white aerial mycelium on plates covered in the familiar orange fruiting bodies (see Fig. 4.5, B).

### 4.3 Targeted gene editing of TA using CRISPR-Cas9

We tried to apply the recently developed CRISPR-Cas9 protocol for TA, by Julia Prinz and Raphael Gabriel (unpublished data), to target genes of interest. Those knockouts would help us to further understand the expression of cellulases in TA.

In section 2.4.1 the CRISPR-Cas9 system and its development for application in filamentous fungi is described in detail. The exact protocol used for our experiments, as well as the structure of the plasmids can be found in section 3.2.5.

#### Targeted Genes and corresponding plasmids

We intended to knock out the following genes with two plasmids each (see Tab. 4.1), varying in the used protospacers and therefore targeting a different region within the gene (for more details on the targeted genes see section 2.2.1).

**Table 4.1.** Targeted genes in the CRISPR-Cas9 experiments and the therefore generated knockout plasmids

Genes	Expected role of the gene	Plasmids
<i>amyR</i>	balancing cellulose and starch utilization	pLF1, pLF2
<i>amdS</i>	acetamidase, allowing the growth on acetamide as sole carbon or nitrogen source	pLF3, pLF4
<i>XlnR</i>	activating the transcription of cellulases and/or hemicellulases	pLF5, pLF6
<i>LPMO</i>	structural gene for the major Lytic Polysaccharide Monooxygenase	pLF7, pLF8
<i>pkaA</i>	important fungal kinase acting on CreA	pLF9, pLF10
<i>creA</i>	master regulator in CCR, downregulating cellulolytic and xylanolytic gene expression	pJP5, pJP6, pJP7

After successfully assembling all 13 CRISPR-Cas9 plasmids (for more details see Tab. 7.2), their integrity was verified with the in-house DIVA sequencing service (see section 3.2.7).

#### Sequencing results of the plasmids

For the CRISPR-Cas9 knockout plasmids the sequencing surprisingly revealed several single nucleotide polymorphisms (SNPs) and inserts. The 13 different plasmids contained on average

7 SNPs, 3 inserts and no deletions. Extensive examination showed that all inserts were due to incorrect mapping to outdated ICE entries and the remaining SNPs were passed along from the template backbone plasmid Bpi1-KO (see Tab. 4.2).

**Table 4.2.** SNPs in the Bpi1 KO plasmid

SNPs	Location on the plasmid
G 2019 A	KanR
T 2963 A	oriV
C 3419 G	oriV
C 5009 T	hph
C 8882 T	Cas9
T 9851 A	Cas9
C 11948 T	SV40

The SNPs in the hygromycin resistance (hph) as well as the kanamycin resistance (kanR) evidently had no effect, as the TA and *E. coli* transformants were still growing on both antibiotics.

To examine whether the mutation in the origin of replication (oriV) had an effect on the plasmid production in *E. coli*, we compared the concentrations of plasmids carrying this mutation, to plasmids with an intact oriV (pJP1 and pJP3). Therefore we performed a miniprep plasmid purification from *E. coli* cultures with the same OD<sub>600</sub> and measured the nucleic acid concentration and purity of the samples with the spectrophotometer. As the concentrations did not vary considerably, we concluded that this point mutation had no effect either.

None of these SNPs seemed to modify the amino acid code of the expressed proteins, but we cannot be sure whether these mutations did not in fact alter translational efficiency of the plasmids.

Sequencing of the plasmids used by Julia Prinz, which were successfully used to generate CRISPR-Cas9 knockouts in TA, showed to have much fewer deviations (only around 4 SNPs and 1 insert). The design of the plasmids was exactly the same but as they seemed to have trouble assembling the 12 kbp backbone plasmid and the comparably small gRNA insert with Gibson assembly, it was decided to use Golden Gate for our experiments. But whether the detected SNPs actually are assembly scars and if these indeed affected the translational efficiency or contributed to the failure of our experiments is still unverified.



### Transformations with the knockout plasmids

The assembled Cas9 plasmids were then used for transformations of TA. Unfortunately, we were not able to generate the Cas9 knockouts by using the protocol that yielded deletion strains before. While the transformation procedure appeared to work quite reliably, we did not get any colonies for most of the tested plasmids. Only transformations with pJP6 and pJP7 (targeting *creA*) reproducibly resulted in colonies, which nonetheless did not seem to carry the aspired mutation. The transformations using other plasmids did not yield colonies.

We performed seven rounds of transformation of TA with *Agrobacterium* carrying the CRISPR-Cas9 knockout plasmids, always including the positive control AB3996. This plasmid generated by Ziyu Dai for *creA* deletion reliably yielded hygromycin resistant colonies before. Unfortunately of the 7 attempts to generate transformants with the 13 different plasmids, only twice did we obtain colonies on the hygromycin-PDA<sub>cefotaxime</sub> selection plates. Only the transformations with plasmids pJP6 and pJP7, both targeting *creA*, resulted in any colonies on hygromycin plates.

### Characterization of putative $\Delta creA$ strains from the CRISPR-Cas9 transformations

The only isolated colonies from the CRISPR-Cas9 gene editing experiments were from transformations with the pJP6 and pJP7 plasmids, both targeting *creA*. Those putative CCR impaired strains were further cultivated on minimal media containing DOG. Putative mutants that seemed to grow better on DOG than the wt (see Fig. 4.6) were isolated and *creA* amplified and sequenced (see Fig. 4.7).

However, these first sequencing results showed to be unreliable and additional DOG media tests were not conclusive.

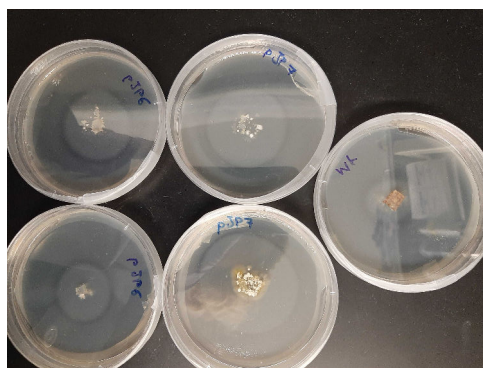


**Figure 4.6.** Growth of some of the isolated putative *creA* mutants on minimal media (soluble starch and yeast extract) with 0.1 % DOG in comparison to the wt.

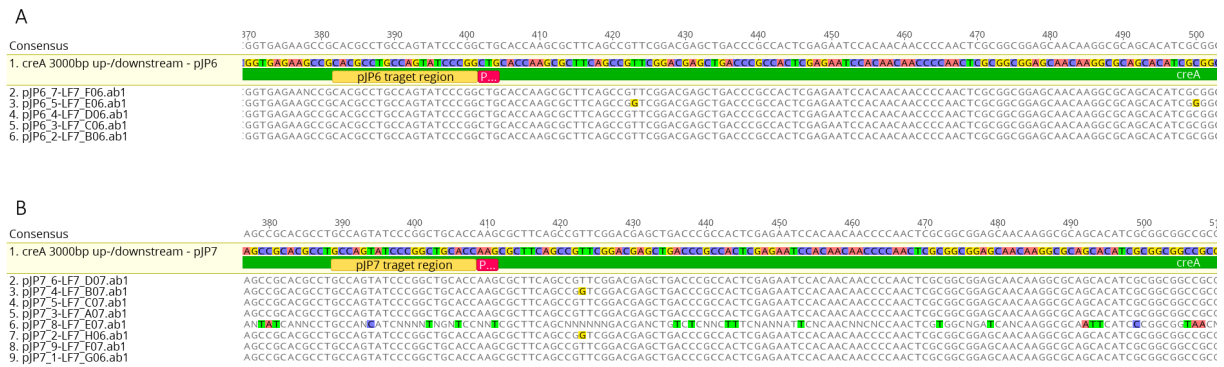


**Figure 4.7.** Sequencing results for *creA* of selected strains from the transformation with pJP6 (A) and pJP7 (B) that indicated a distorted CCR. The protospacer target region is marked in yellow and the PAM sequence in pink. Notably only four strains (pJP7\_4, pJP7\_2, pJP6\_5 and pJP6\_1a) exhibit point mutations. Generated with Geneious Prime [1].

From the chosen strains, only four had substitutions of single bases in vicinity of the targeted region. Prior gene knockouts with CRISPR-Cas9 in TA resulted in massive deletions and frame-shift mutations close to the PAM site. But due to the still significantly better growth on DOG in comparison to the wt, we decided to continue investigating the four putative  $\Delta creA$  strains (pJP7\_4, pJP7\_2, pJP6\_5 and pJP6\_1a).

To quantitatively compare the growth of the mutants to the TA wt, we tested various carbon sources (D-xylose, soluble starch with yeast extract, oatmeal agar) and increasing DOG concentrations (0 - 0.2 %).

Wt cells with an active *creA*, regulating the up-take of a preferred carbon source, will primarily utilize the sugar analog 2-deoxy-D-glucose (DOG) which blocks further glycolysis, leading to the starvation of the cell.  $\Delta creA$  strains however are more resistant as they more readily metabolize other complex sugars.

The used carbon sources were chosen based on experience and additional prior experiments. Growth of the TA wt on oatmeal usually yields high amounts of spores and the fungus grows very quickly and dense (see Fig. 4.8, A. middle).

TA also grows well on soluble starch (SS). Soluble starch however showed to be problematic upon the addition of DOG, as the wt hardly continued to grow even at very low DOG concentrations. We therefore investigated the addition of different nitrogen sources (see Fig. 4.8, B). Especially the addition of 1 g/L yeast extract (YE) made the wt grow much better even under higher

DOG concentrations. This might be because yeast extract does not only enrich the medium with vitamins and amino acids, but also additional carbohydrates.

D-xylose is known to induce the production of cellulases in TA [40]. The fungus grows in tick white patches and relatively early produces spores (see Fig. 4.8).

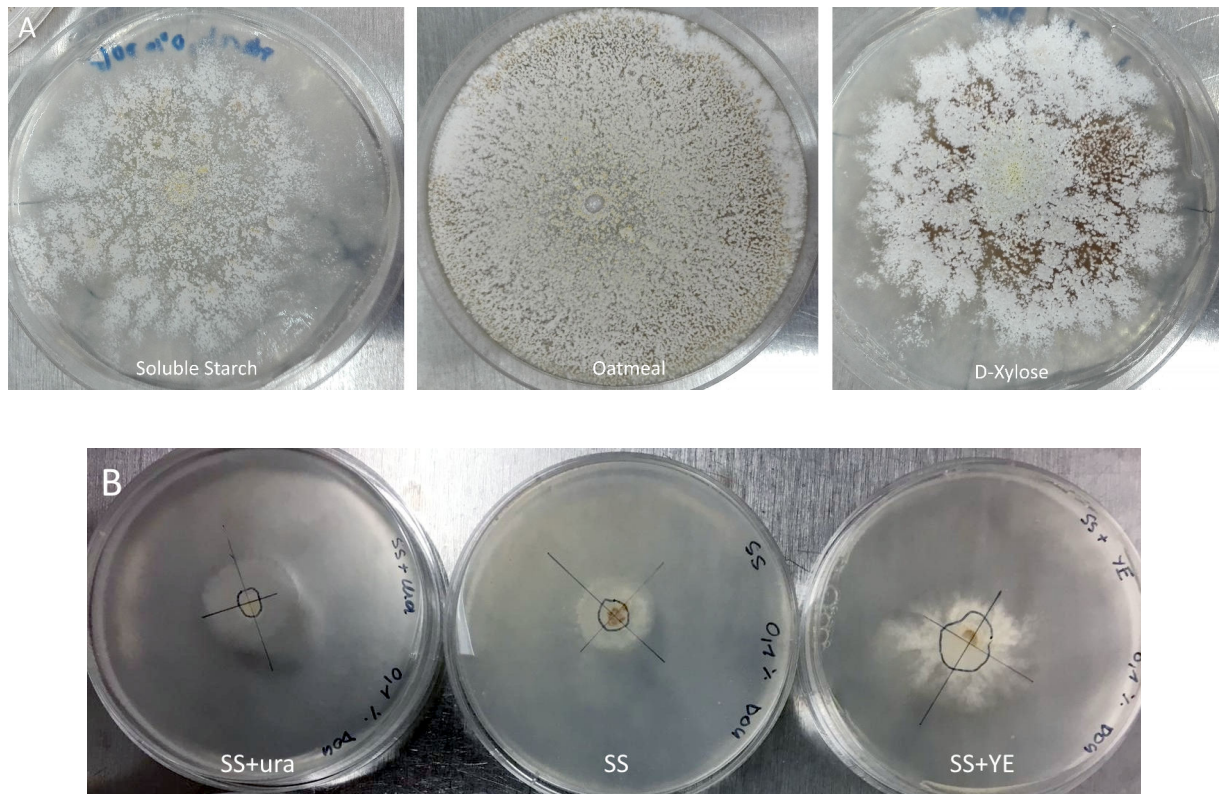


**Figure 4.8. A.** Growth of TA wt after 3 days on minimal media, without DOG, on different carbon sources: soluble starch (left), oatmeal (middle) and D-xylose (right).

**B.** Growth of TA wt after one week on minimal media with soluble starch and 0.05 % DOG, but with additional nitrogen sources: uracil (ura, left), none (middle) and yeast extract (YE, right).

After deciding on the media, the four putative  $\Delta creA$  strains and the wt were grown for 3 days, before the colony diameter was measured with a vernier caliper diagonally twice and averaged (see Fig. 4.9).

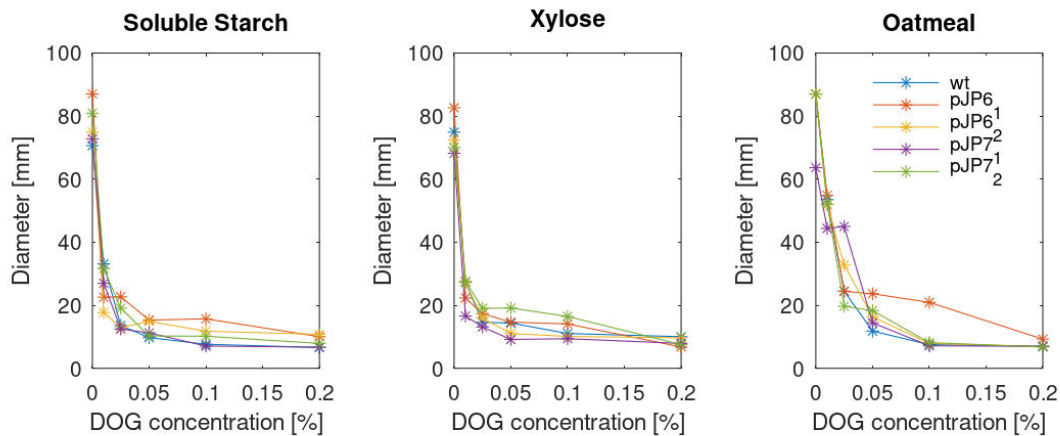


**Figure 4.9.** Growth of putative *creA* deletion mutants in comparison to the wt on minimal media with DOG (soluble starch with yeast extract, D-xylose and oatmeal agar), to screen for strains lacking carbon catabolite repression, which is mediated by *creA*.

After initially receiving promising sequencing results, a single base insert within the protospacer binding region, indicating a successful Cas9 cut, as well as distinctive growth on DOG - further results were rather disillusioning. As can be seen on Fig. 4.9, the growth on increasing DOG concentrations could in fact not be distinguished from the wt. pJP6<sub>1</sub> seems to have a slightly better growth, especially on Oatmeal agar with a DOG concentration of 0.1 % 4.9. However, Oatmeal agar is very dense which makes it harder to accurately measure the diameters of the colonies.

As the DOG growth tests were not conclusive, we performed additional sequencing of the strains used, which surprisingly showed a completely functional *creA* (see Fig. 4.10).

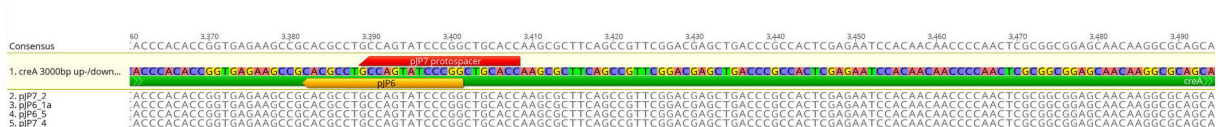


**Figure 4.10.** Sequencing results for *creA* of the thought to be  $\Delta creA$  strains show a functional gene without any mutations. Notably this figure shows the same segment of the gene as in Fig. 4.7. Generated with Geneious Prime [1].

Further experiments might determine if pJP6<sub>1</sub> actually is carbon catabolite derepressed, and if this is the case what causes this, as the strain had an active *creA*.

---

## 5 Discussion

### 5.1 Random mutagenesis

Our goal for the random mutagenesis experiments to obtain the desired mutant strains was met, though the collateral background mutations showed to be problematic.

All strains selected on FAA had a mutant *amdS* gene, while not all of the carbon catabolite derepressed strains selected on DOG seemed to have a mutated *creA*. In these random mutagenesis experiments we did not yield any  $\Delta pyrE / pyrG$  colonies from the selection on 5-FOA plates, however this was already successfully realized in earlier experiments by Raphael Gabriel.

Therefore it can be concluded that random mutagenesis is a very efficient method to generate mutant TA strains. The developed protocol does not require elaborate equipment, nor is it time- and labor-intensive.

The main constraints for this method are the limited number of genes one can select for and the tedious subsequent screening of generated mutants. In our experiments with UV radiation and EMS, the retrieved strains generally contained too many mutations and often heavily distorted phenotypes (e.g. very dense white aerial mycelium or no spore formation).

#### **Attempts to generate a carbon catabolite derepressed strain**

Historically researchers very successfully used random mutagenesis in combination with suitable selection regimes for strain development. A classic example thereof is the development of the *Trichoderma reesei* hypersecreting strain RUT-C30. It was obtained by three rounds of mutagenesis (twice with UV and once with N-methyl-N'-nitro-N-nitrosoguanidine) and is commonly used for the production of cellulases, attaining more than 30 g/L in industrial fermentation [43]. RUT-C30 was selected on 2-deoxyglucose (DOG) to screen for strains with impaired carbon catabolite repression (CCR). Later it was discovered that a mutation in the key transcription regulator *cre1* (in TA *creA*) was mainly responsible for the carbon catabolite derepression and cellulase hyperproduction.

Interestingly random mutagenesis to generate hyperproducing strains e.g. in *Myceliophthora thermophila* drastically lowered the viscosity of the liquid culture (by 50-fold) due to the altered mycelial morphology [49]. This is a very intriguing side effect, as the viscosity in the liquid culture of filamentous fungi commonly is a big obstacle, as it i.a. strongly reduces the oxygen

and nutrient transfer [49].

We attempted to imitate this method to generate a *creA* deletion strain by mutating and selecting on DOG.

Most of the sub-cultivated colonies, picked from the DOG selection plates, did not grow as well as the wt on regular minimal media or PDA. *creA* is not only a key transcription regulator, affecting the carbon metabolism, but also involved in the development of conidia and hyphae [26], which commonly led to growth defects in recombinant *creA* deletion strains. Unfortunately we did not follow up on the growth behavior or cellulase production of the putative carbon catabolite derepressed strains obtained from random mutagenesis.

Nevertheless, the generation of a carbon catabolite derepressed strain should be possible also for TA. Presumably a reduction of the UV or EMS exposure time, using less DOG or a different screening procedure in the first selection step but increasing its concentration for the secondary selection, and radically increasing the scale of the experiments could lead to success.

### **Attempts to generate a $\Delta amdS$ strain**

The strains derived from selection on FAA however, all showed to have at least one mutation within the *amdS* gene. Despite this first favorable outcome, their heavily varying phenotypes, with some of them not producing spores anymore, revealed undesired side effects of the mutagenesis treatment.

In an attempt to retrieve a more typical phenotype, we tried to backcross these obtained  $\Delta amdS$  strains with the wt (for this discussion, see section 5.2).

## **5.2 Sexual crossing**

Sexual crossing in TA showed to be very simple and reliable. All tested progeny of the crossed strains exhibited the assessed traits from both parent strains. Regarding the crossing of  $\Delta ku70$  and  $\Delta pyrE$  (strain 45-3) for example, resulted in a population with hygromycin resistance inherited from the  $\Delta ku70$  and an impaired *pyrE* from the 45-3.

The availability of this method alone is a greatly beneficial for working with this organism.

### **Crossing of $\Delta ku70$ and $\Delta pyrE$**

Crossing of the NHEJ-impaired  $\Delta ku70$  and the  $\Delta pyrE$  strain 45-3 were very promising, and we tested their growth on minimal media selecting for the desired traits (see Fig. 4.3).

All of the obtained crossed strains were resistant to hygromycin, which was inherited from the  $\Delta ku70$  strain, but also to 5-FOA, indicating the uracil auxotrophy arising from the inherited impaired *pyrE*. The *pyrE* gene of the crossing progeny was sequenced, showing a coinciding, hereditary SNP from the original  $\Delta pyrE$  strain.

### Mutations in the $\Delta ku70$ strains

The subcultivars as well as the cryo stock of the  $\Delta ku70$  strain exhibited mutations in the *pyrG* gene, explaining their unexpected growth on 5-FOA. We therefore concluded that the knockout of *ku70* in TA supposedly leads to grave genomic instability, enabling these spontaneous and random mutations and that this strain might not be as stable as anticipated.

The extent to which an organism is effected by a disrupted *ku70* or *ku80* can vary drastically, depending on the species. *Penicillium digitatum* with an inactivated *ku70* for example showed absolutely no differences to the wt until it was grown at a slightly higher temperature, heavily effecting its growth and conidia production [15]. For the basidiomycete *Ustilago maydis* however it was shown that both Ku proteins are absolutely essential for cell viability and a disruption lead to a complete arrest of the cell cycle, stopping any proliferation [9].

It would certainly be interesting to further investigate the extent to which the  $\Delta ku70$  TA strain is mutated. Alternatively, it might be helpful to assess if incubations at lower temperatures (< 45 °C) lead to more strain stabilities, since incubations at higher temperature increases cell metabolism and thus could lead to more mutations over time.

### Crossing of $\Delta amdS$ and wild type

Attempts to back-cross  $\Delta amdS$  strains generated with random mutagenesis with the wt to reduce the overall number of mutations in the genome showed to be quite challenging.

In some cases this certainly was caused by the insufficient or completely impaired spore production of some of the mutants. Some of our crossing attempts worked, as we received strains that were still growing on FAA and had a phenotype closer to the wt.

Most of the cultivars however did not grow well and due to the expected ubiquity of mutations we decided to discontinue further experiments with those strain, as it seems hard to estimate how they will behave.

To determine the proximity of the from the crossing obtained cultures to the wt was only done by visual inspection and assessment of the phenotype. Alternative methods to investigate this closeness would involve extensive sequencing e.g. double digest restriction site associated

DNA sequencing (ddRADseq), to map all single SNPs to the wt genome and to gain a deeper understanding of the underlying genetic basis for observed variations in phenotype and morphology [19].

An interesting approach to increase the outcrossing rate was described in the facultative sexual *A. nidulans*. By adding a non-lethal fungicide, and thereby creating a stressful environment for the strains to be crossed, researchers could obtain progeny with a higher fitness [31]. It would be interesting to see whether e.g. in the case of  $\Delta amdS$  x wt, the addition of FAA in a low concentration to the media on which the strains grow together, would increase the reshuffle of the genome.

### 5.3 CRISPR-Cas9 gene knockouts

Targeted gene knockout in TA showed to be more challenging than expected. Julia Prinz and Raphael Gabriel demonstrated the functionality of this CRISPR-Cas9 plasmid design in *Aspergillus niger* to knockout the *albA* gene, as well as successfully targeting the *pyrG* in TA (unpublished). Although a very low transformation efficiency was reported, the protocol seemed ready to be applied to different genes in TA. Ultimately we did not receive any verified and stable knockout strains of the targeted genes.

In the following sections we will list and discuss some of the problems and challenges we encountered in the attempt to perform CRISPR-Cas9 gene knockouts in TA.

#### SNPs in the plasmids

As we ordered the individual protospacer-cassettes as a synthesized gBlock (IDT), and then assembled these oligos via the efficient and usually seamless Golden Gate cloning with a common backbone plasmid, we expected the plasmids to be basically error free.

However sequencing revealed some alarming SNPs, two of them within the gene sequence of the Cas9 and one in the SV40. Even though *in silico* these alterations do not seem to have an effect on the amino acid code, we cannot exclude that they cause a malfunction of the Cas9 or an insufficient translocation to the nucleus.

As our constructs had the same basic design as the ones successfully used by Julia Prinz, it seems likely that the found SNPs are caused by the method of assembly. Previously a Gibson assembly was used, which showed to be problematic due to the size difference of the insert (few hundreds base pairs) and size of the vector (app. 12 kbp). By using Golden Gate with designated base pair overhangs to guarantee correct assembly and systematically integrated restriction enzyme



cut sites as designed with DIVA (j5 DNA Assembly Design Automation Software) [20], we did not encounter any of the previously reported problems during plasmid assembly.

The origin of these SNPs, which might be caused by the assembly process, or their impact on the general functionality of the plasmids remain unanswered.

### **Lack of colonies after transformation**

*Agrobacterium* mediated transformation (AMT) worked in TA before, as we obtained colonies from the transformation with the *hph*-positive control. Experiments by Julia Prinz however demonstrated that transformation efficiencies can vary depending on the used plasmid. AMT in TA is a delicate process based on a highly fine tuned protocol. Any deviation, e.g. of the pH of the induction media or the temperature during coincubation, could potentially lead to failure. Even though it therefore frequently occurs that the transformation procedure does not work as planned, our success rate was unexpected low.

We tested all 13 constructed plasmids, each at least twice, but only obtained colonies from the transformation with pJP6 and pJP7, both targeting *creA*. Whether it is a coincidence that the only two plasmids that worked, actually target the same gene, is questionable. It would be understandable if the plasmids targeting a structural gene e.g. for the LPMO, would work better, as impairing a key transcriptional factor like *creA* often can be devastating for a cell.

To reduce the possibility of human failure, we repeated the experiments several times, with different operators handling different steps in the procedure. We double checked the temperature controls of the incubators, measured the pH of each medium twice, used different batches of material.

Interestingly Foster et al. encountered a similar problem in 2017, although naturally their setup is not completely comparable to ours (e.g. usage of protoplasts, different organism).

Another group seemed to have established a functional CRISPR-Cas9 system in *Magnaporthe oryzae* [5], which even when using the same constructs showed to not be reproducible [14]. They noticed however that transformations with constructs whether with or without any gRNA present but carrying the Cas9-encoding sequence resulted in far fewer colonies than empty vector controls [14].

As already demonstrated in yeast, the stable expression of Cas9 can be very toxic to some organisms and could therefore lead to lack of colonies upon transformation [23]. Foster et al. subsequently developed a ribonucleoprotein-CRISPR-Cas9 (RNP-CRISPR-Cas9) system which uses *in vitro* synthesised sgRNA and purified nuclear-localised Cas9 to avoid genomic integration

and constant expression of Cas9 inside the fungal cell [14].

Another approach described is the usage of a deactivated Cas9 (dCas9) to simply block gene expression [10]. dCas9 still binds the DNA through the guidance of the sgRNA, but instead of cutting the double strand, it sterically hinders the RNA polymerase to elongate that gene [41]. Despite the infancy of this method, it was successfully applied in several bacterial species to elucidate their physiology or in metabolic engineering [41]. In 2019 Wensing et al. first demonstrated its application for the first time in a fungal pathogen (*Candida albicans*), obtaining an app. 20 fold transcription repression of the targeted gene [50].

Follow-up experiments regarding the targeted gene knockout in TA should definitely test for the toxicity of Cas9, using the same constructs but with a disrupted nuclease. Point mutations in one of the two catalytic domains of Cas9 lead to a variant cutting only one DNA strands (nickase), while mutating both provides the mentioned dCas9 [12]. Both strategies could be implemented with designed oligos and PCR targeting the catalytic site.

### Characterizations of the putative $\Delta creA$ strains

The characterization of the few putative carbon catabolite derepressed strains from AMT showed to be quite astonishing. After the first sequencing results indicating at least single base exchanges in four strains we zealously started the tests for growth on DOG in comparison to the wt. As they did not exhibit any divergent growth behavior, we sequenced these four strains again and to our great surprise found a completely intact *creA*.

CRISPR-Cas9 knockouts by Julia Prinz exhibited massive frameshift mutations within the targeted genes. But as already the amplification of *creA* showed to be challenging (we tried different primer combinations), we expected this gene to be especially well protected and little accessible.

The first sequencing results of the obtained colonies were already nonsatisfying, as they showed to be only single base exchanges and were not in the expected region where the Cas9 would cut (within the PAM sequence, see Fig. 4.7). Additionally these mutations did not seem to be stop codons or frame shift mutations, which makes it unlikely that they lead to a loss of function in *creA*.

This sudden resurgence of the functional gene shown in the second sequencing, however might also be explained by the homothallic nature of TA and the heterogeneous mixture of different genotypes present in the obtained colonies after transformation. The CRISPR-Cas9 system is still in an early period of development and implementation in filamentous fungi and had has only

been established in a limited number of species. One of the main problems is feasibility, as the workload needed to select for positive clones is enormous. Therefore researchers prefer to target functional genes effecting the transformants phenotype [46]. A prominent example therefore is the knockout of the common phenotypic marker gene *albA* in *Aspergillus* species, which leads to white instead of the normal black spore pigmentation [32].

Screening for single spores with knocked out genes, which do not result in any phenotypic aberration, but which mutation might strongly impact the growth, as e.g. was observed in some  $\Delta cre1$  strains of *T. reesei* [43], therefore is highly labor-intensive.

Additionally, strains with a hygromycin resistance, but without further mutations seem to be fitter and propagate better. Outcrossing events allow this genotype then to dominate the colony.

Single cells with an impaired *creA* would not show a differentiable phenotype, and would be impossible to visually screen for. Possibly a higher DOG concentration than the used 0.1 %, as a secondary selection step right after the transformation would be beneficial to hinder the growth of carbon catabolite repressed cells.

In principle the screening with DOG should work well, as it was successfully used to screen for carbon catabolite derepressed strains in e.g. *N. crassa* [4], *T. reesei* [43] and *M. thermophila* [49]. In the screening for carbon catabolite derepressed strains after random mutagenesis we saw that some putative  $\Delta creA$  strains seemed to have a significant better growth than the wt on DOG. However, more testing is needed to determine if the selection on DOG is working well for TA or whether a cellulase secretion screening would be more helpful.

Overall we did not succeed in the generation of any stable knockout strains of TA with CRISPR-Cas9. Whether this was due to faulty plasmids, undiscovered errors or inefficacy of the applied transformation protocol, or other unknown factors could not be determined. To generate the desired knockouts, and to investigate the specific reasons for our disappointing results, the next steps would definitely include experiments testing the toxicity of Cas9 in TA, PCRs to correct the SNPs in the plasmids and probably another in depth analysis on parameters that could increase the AMT efficiency.

## 6 Conclusion

Our goal was to expand our knowledge regarding the methods and procedures used to manipulate the genome of TA.

We experimented with random mutagenesis by UV radiation and with EMS and successfully generated large numbers of *amdS* and *creA* deletion mutants on some of the chosen selection plates. Screening of putative mutants carrying the desired traits however showed to be labor-intensive and would require high throughput systems for liquid cultivation and the subsequent proteomic analysis. Moreover, further trials applying different concentrations of the selection substances or the exposure times could lead to a greater variety of mutants.

The protocol for sexual crossing worked reliably. Notably, as with the mutagenesis, we are limited to characteristics we can screen and select for. The ability to stack mutations certainly is a big advantage for working with TA, but more research should eventually go into further fine tuning this useful protocol.

Targeted gene editing in TA is still challenging. With *Agrobacterium* mediated transformation, there is finally a relatively steady protocol to transfer plasmids into TA. However, attempts to simplify this procedure regarding the labor input and required time would most likely be rewarded.

The tested CRISPR-Cas9 system had in the past already been successfully used to knockout *pyrG* in TA (unpublished data). However, our experiments did not yield conclusive evidence for deletion of the genes targeted in this work. We detected a variety of putative reasons for this failure but were not able to definitively determine the true technical or human error causing our problems with transforming and isolating strains. This leaves us with a long list of suggested next steps to improve or enable this procedure. The most imminent ones seem to be testing the toxicity of Cas9 in TA and to further verify the functionality of our generated plasmids.

Overall, though we did not generate stable new mutant strains, we were able to gain more insight into working with TA, leaving us with a deeper understanding on technical challenges and ideas for benefiting future projects.

## 7 Appendix

### 7.1 Abbreviations

**Table 7.1.** List of all abbreviations used

<b>Abbreviation</b>	<b>Explanation</b>
5-FOA	5-fluoroortic acid
A	Adenine
AA	Auxiliary Activities family
AMT	<i>Agrobacterium</i> mediated transformation
app	Approximately
Ara	Arabinose
ATCC	American Type Cell Culture Collection
ATP	Adenosine triphosphate
BGG	Bovine Gamma Globulin
bp	Base pair(s)
C	Cytosine
Cas9	CRISPR-related nuclease 9
CAZy	Carbohydrate Active enZymes
CBM	Carbohydrate-Binding Module Family
CCR	Carbon catabolite repression
CE	Carbohydrate Esterase family
cm	Centimeter
Cm	Chloramphenicol
CMC	Carboxymethyl cellulose
CRISPR	Clustered regularly interspaced short palindromic repeat
crRNA	CRISPR RNA
ddRADseq	Double digest restriction site associated DNA sequencing
DE	Differentially expressed
DIVA	Design, Implementation, and Validation Automation
DOG	2-deoxy-D-glucose
eg	Example given
ER	Endoplasmatic reticulum
ERAD	ER-associated degradation

<b>Abbreviation</b>	<b>Explanation</b>
F	Farad
FAA	Fluoroacetamide
g	Gram
G	Guanine
gDNA	Genomic DNA
GFP	Green fluorescent protein
GH	Glycoside Hydrolase
GH	Glycoside Hydrolase family
Glu	Glucose
GO	Gene Ontology
GT	Glycosyl Transferase family
hph	Hygromycin resistance
HR	Homologous recombination
HTS	High throughput screening
ICE	Inventory of Composable Elements
IDT	Integrated DNA Technologies
JGI	Joint Genome Institute
Kann	Kanamycin
KEGG	Kyoto Encyclopedia of Genes and Genomes
KOG	EuKaryotic Orthologous Groups
kV	Kilo volt
L	Liter
L0	Level Zero
LB	Lysogeny broth
M	Molar
MES	2-(N-morpholino)ethanesulfonic acid
NC	No carbon
NCBI	National Center for Biotechnology Information
NEB	New England Biolabs
NGS	Next Generation Sequencing
NHEJ	Non-homologous end-joining
OD	Optical density
PAGE	Polyacrylamide gel electrophoresis

<b>Abbreviation</b>	<b>Explanation</b>
PAM	Protospacer Adjacent Motif
PCA	Principal Component Analysis
PCR	Polymerase Chain Reaction
PDA	Potatoe dextrose agar
PDA	Potatoe dextrose agar
pID	Protein ID
PMT	Protoplast-mediated transformation
QC	Quality control
rpm	Rounds per minute
SDS	Sodium dodecyl sulfate
sgRNA	Single guide RNA
SNP	Single Nucleotide Polymorphism
SS	Soluble Starch
T	Thymine
TA	<i>Thermoascus aurantiacus</i>
TCDB	Transporter classification database
tID	Transcript ID
tracrRNA	Trans-activating crRNA
U	Units
UPR	Unfolded protein response
vst	Variance stabilizing transformation
wt	Wild type
Xyl	Xylose
YE	Yeast Extract

## 7.2 Plasmids

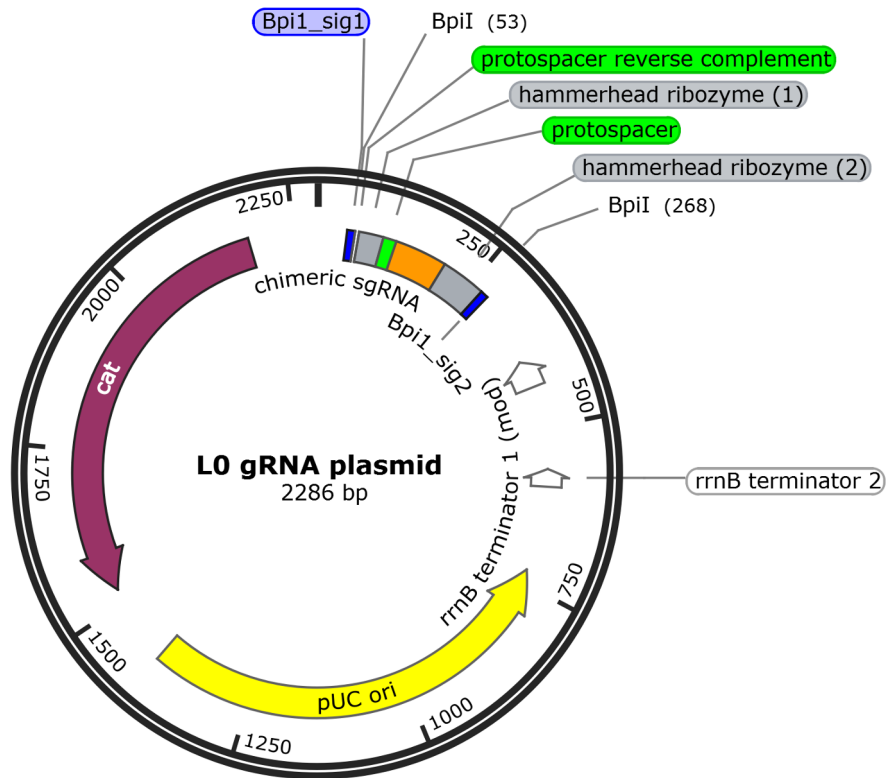


Figure 7.1. Map of the L0 gRNA plasmid, created with the SnapGene Software [42].

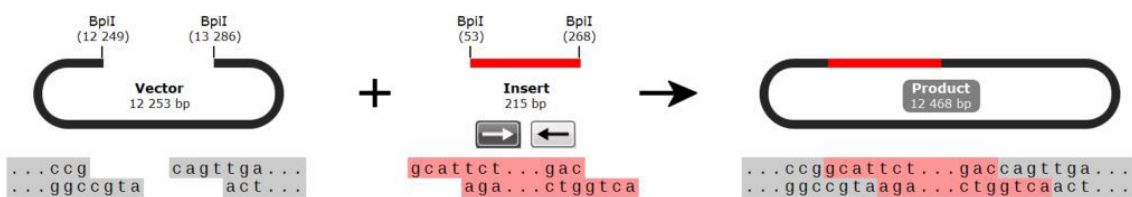
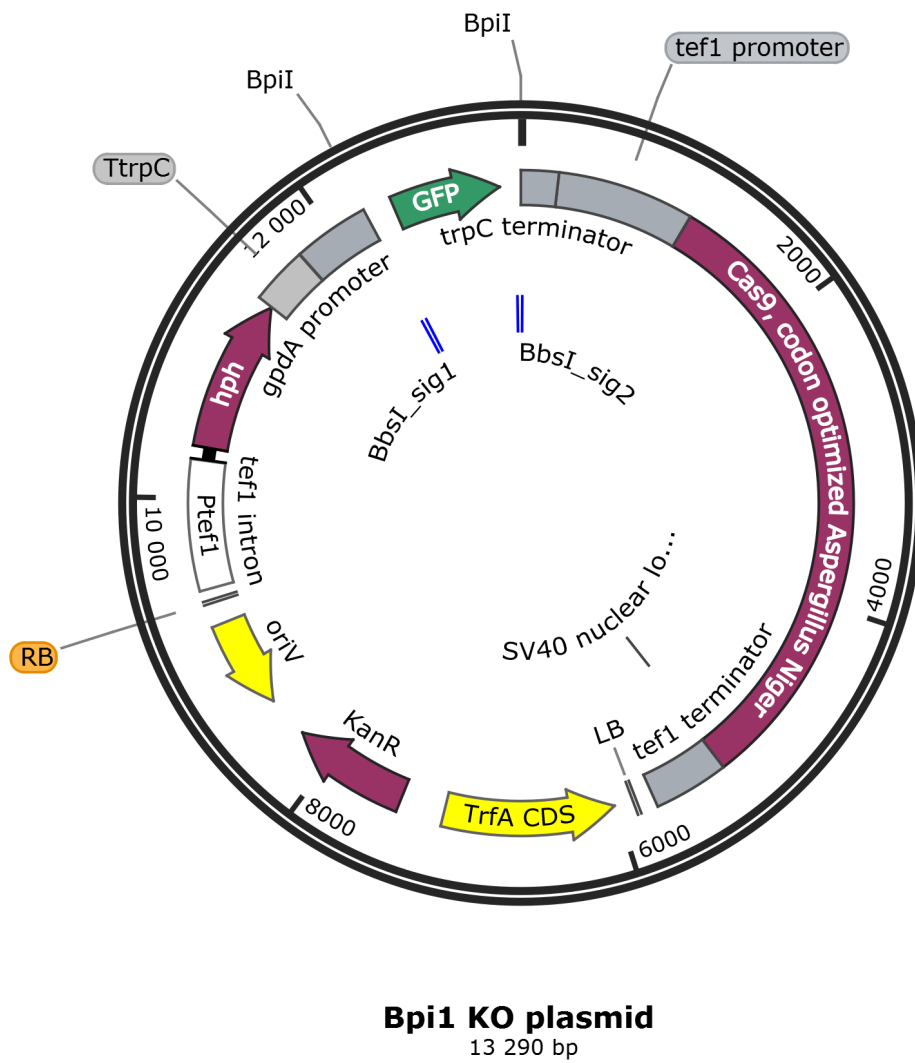
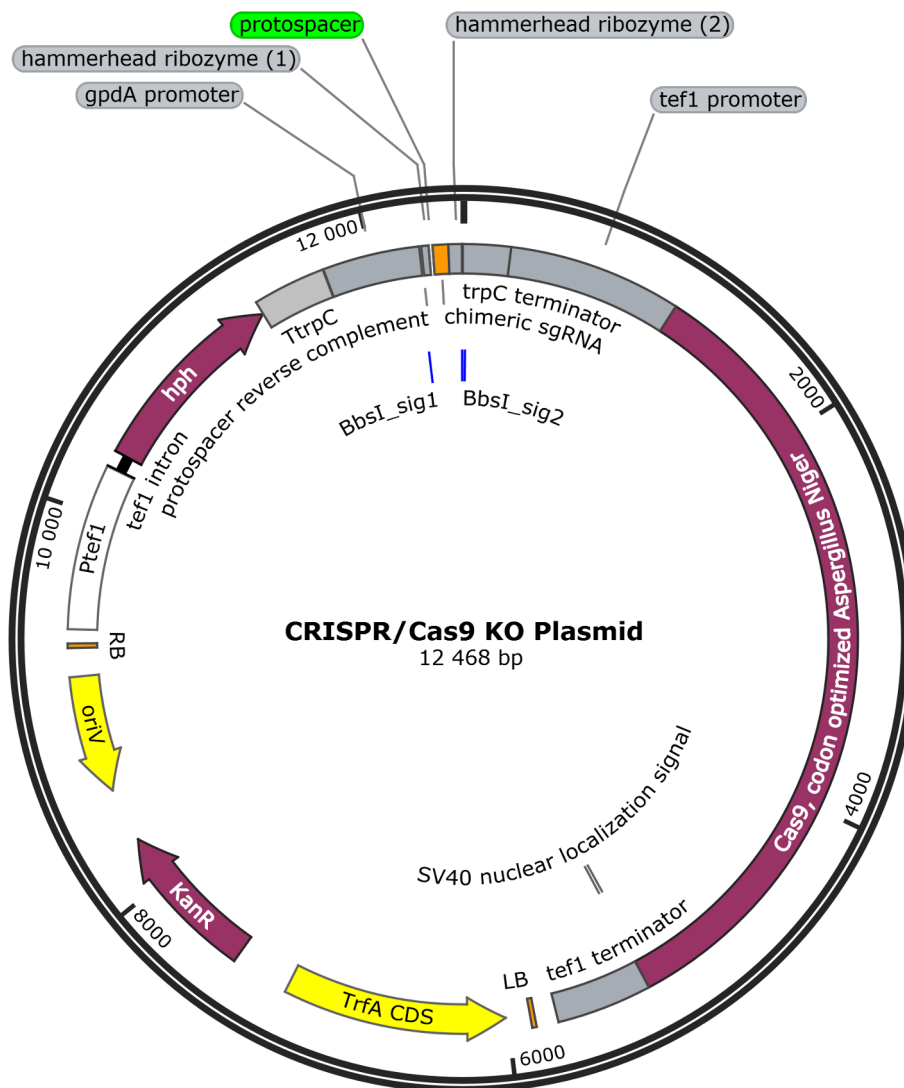


Figure 7.2. Schema of the specific 4 bp overhangs created by the restriction enzyme and their utilization in Golden Gate Cloning (created with the SnapGene Software [42]).





**Figure 7.3.** Map of the Bpi1 KO plasmid, created with the SnapGene Software [42].



**Figure 7.4.** Map of the CRISPR/Cas9 Knockout Plasmid, created with the SnapGene Software [42].

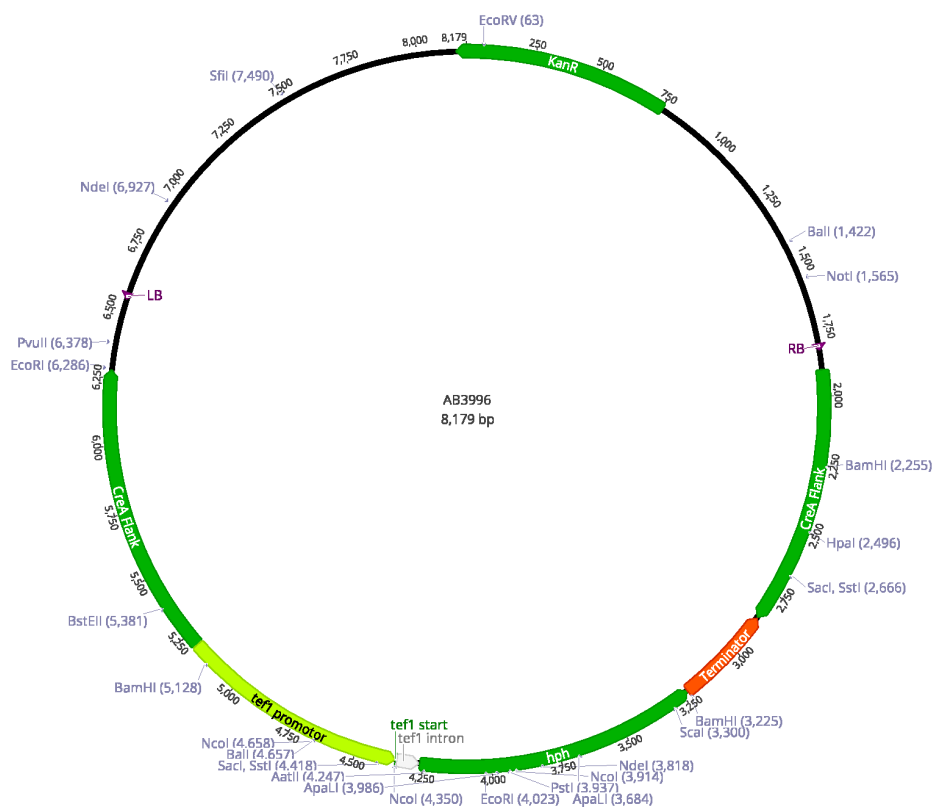


**Figure 7.5.** Map of the AB3996 Plasmid created by Ziyu Dai, used as a positive control for the AMT in TA (map generated in Geneious Prime [1]).

**Table 7.2.** All assembled plasmids – properties and application  
(Cm...chloramphenicol , Kan...kanamycin, hph...hygromycin, GFP... green fluorescent protein)

Plasmid	Assembly	marker		Parent	Information
		<i>E. coli</i>	Fungal		
gRNA_L0_1	Gibson	Cm	-	pSTART_chlor	L0 gRNA for pLF1, synthetic gRNA cassette
gRNA_L0_2	Gibson	Cm	-	pSTART_chlor	L0 gRNA for pLF2, synthetic gRNA cassette
gRNA_L0_3	Gibson	Cm	-	pSTART_chlor	L0 gRNA for pLF3, synthetic gRNA cassette
gRNA_L0_4	Gibson	Cm	-	pSTART_chlor	L0 gRNA for pLF4, synthetic gRNA cassette
gRNA_L0_5	Gibson	Cm	-	pSTART_chlor	L0 gRNA for pLF5, synthetic gRNA cassette
gRNA_L0_6	Gibson	Cm	-	pSTART_chlor	L0 gRNA for pLF6, synthetic gRNA cassette
gRNA_L0_7	Gibson	Cm	-	pSTART_chlor	L0 gRNA for pLF7, synthetic gRNA cassette
gRNA_L0_8	Gibson	Cm	-	pSTART_chlor	L0 gRNA for pLF8, synthetic gRNA cassette
gRNA_L0_9	Gibson	Cm	-	pSTART_chlor	L0 gRNA for pLF9, synthetic gRNA cassette
gRNA_L0_10	Gibson	Cm	-	pSTART_chlor	L0 gRNA for pLF10, synthetic gRNA cassette
gRNA_L0_11	Gibson	Cm	-	pSTART_chlor	L0 gRNA for pJP5, synthetic gRNA cassette
gRNA_L0_12	Gibson	Cm	-	pSTART_chlor	L0 gRNA for pJP6, synthetic gRNA cassette
gRNA_L0_13	Gibson	Cm	-	pSTART_chlor	L0 gRNA for pJP7, synthetic gRNA cassette
KO_synth_creA	Gibson	Kan	hph	pJP4	Knockout Plasmid (synthetic gRNA) for creA from pJP5
KO_Bpi1	Gibson	Kan	GFP	pJP4, pTS57	KO Plasmid backbone with a GFP reporter

Plasmid	Assembly	marker		Parent	Information
		<i>E. coli</i>	Fungal		
pLF1	Golden Gate	Kan	hph	gRNA_L0_1, KO_Bpil	Plasmid to knockout amyR with CRISPR/Cas9 in TA
pLF2	Golden Gate	Kan	hph	gRNA_L0_2, KO_Bpil	Plasmid to knockout amyR with CRISPR/Cas9 in TA
pLF3	Golden Gate	Kan	hph	gRNA_L0_3, KO_Bpil	Plasmid to knockout amdS with CRISPR/Cas9 in TA
pLF4	Golden Gate	Kan	hph	gRNA_L0_4, KO_Bpil	Plasmid to knockout amdS with CRISPR/Cas9 in TA
pLF5	Golden Gate	Kan	hph	gRNA_L0_5, KO_Bpil	Plasmid to knockout XlnR with CRISPR/Cas9 in TA
pLF6	Golden Gate	Kan	hph	gRNA_L0_6, KO_Bpil	Plasmid to knockout XlnR with CRISPR/Cas9 in TA
pLF7	Golden Gate	Kan	hph	gRNA_L0_7, KO_Bpil	Plasmid to knockout LPMO with CRISPR/Cas9 in TA
pLF8	Golden Gate	Kan	hph	gRNA_L0_8, KO_Bpil	Plasmid to knockout LPMO with CRISPR/Cas9 in TA
pLF9	Golden Gate	Kan	hph	gRNA_L0_9, KO_Bpil	Plasmid to knockout pkaA with CRISPR/Cas9 in TA
pLF10	Golden Gate	Kan	hph	gRNA_L0_10, KO_Bpil	Plasmid to knockout pkaA with CRISPR/Cas9 in TA
pJP5	Golden Gate	Kan	hph	gRNA_L0_11, KO_Bpil	Plasmid to knockout creA with CRISPR/Cas9 in TA
pJP6	Golden Gate	Kan	hph	gRNA_L0_12, KO_Bpil	Plasmid to knockout creA with CRISPR/Cas9 in TA
pJP7	Golden Gate	Kan	hph	gRNA_L0_13, KO_Bpil	Plasmid to knockout creA with CRISPR/Cas9 in TA

## 7.3 Media

### Induction Media

**Table 7.3.** Liquid induction media used for the *Agrobacteria* mediated transformation of TA

Reagent	Volume [mL]
20X AB salt solution	50.0
500 mM phosphate solution	2.4
50X MES-Buffer	20.0
10 % thiamine	0.1
36 % glucose	5.5
100 mM acetosyringone	2.0
water	920.0

**Table 7.4.** Solid induction media used for the *Agrobacteria* mediated transformation of TA

Reagent	Volume [mL]
20X AB salt solution	50.0
500 mM phosphate solution	2.4
50X MES-Buffer	20.0
10 % thiamine	0.1
36 % glucose	5.5
100 mM acetosyringone	2.0
1.5 % Bacto Ager	15.0 g
water	480.0

## 7.4 Buffers and solutions

**Table 7.5.** 20X AB salt solution as used for the liquid and solid induction media

Reagent	Amount [g]
Ammonium chloride	10.0
Magnesium sulfate heptahydrate	3.0
Potassium chloride	1.5
Calcium chloride	0.1
Iron (II) sulfate heptahydrate	0.0075

**Table 7.6.** 500 mM phosphate solution as used for the liquid and solid induction media (pH 7.5)

Reagent	Amount [g]
Dibasci potassium phosphate	30
Sodium phosphate monobasic	10

**Table 7.7.** MES buffer as used for the liquid and solid induction media (pH 5.5)

Reagent	Amount [g]
MES 2X	7.8
MES 50X	195.0

**Table 7.8.** DNS reagent used in the DNS assay. DNS and NaOH are dissolved in 300 mL water, sodium potassium tartrate is dissolved in 300 mL as well - both solutions are combined and filled up to a final volume of 1 L.

Reagent	Amount [g]
3,5-Dinitrosalicylic acid	10
NaOH	16
sodium potassium tartrate	300

**Table 7.9.** McClendon's media component I: notably mixing of salt solution A and B directly would lead to precipitation, adjust to pH 5.0 and bring to 1 L

Reagent	Amount [mL]
50X McClendon salts A	20
25X McClendon salts B	40
500X trace element solution	2
dH <sub>2</sub> O	800

**Table 7.10.** McClendon's salt solution A (Na, Mg, Ca, Cl), bring to 1 L

Reagent	Amount [mL]	Final conc. in 1X [mM]
dH <sub>2</sub> O	600	
NaCl	100 g	34
1 M MgCl <sub>2</sub> *6H <sub>2</sub> O	125	2.5
1 M CaCl <sub>2</sub> *2H <sub>2</sub> O	35	0.7

**Table 7.11.** McClendon's salt solution B (Phosphate salts), bring to 1 L and pH 5.0

Reagent	Amount [mL]	Final conc. in 1X [mM]
dH <sub>2</sub> O	600	
KH <sub>2</sub> PO <sub>4</sub> (monobasic)	75 g	11
KH <sub>2</sub> PO <sub>4</sub> (dibasic)	50 g	5.5

**Table 7.12.** McClendon's trace elements: adjusted to pH 1.0 - 1.7 with H<sub>2</sub>SO<sub>4</sub>

Reagent	Amount [g]
dH <sub>2</sub> O	200 mL
ZnSO <sub>4</sub> *7H <sub>2</sub> O	0.15
MnCl <sub>2</sub> *4H <sub>2</sub> O	0.79
FeSO <sub>4</sub> *7H <sub>2</sub> O	0.11
CoCl <sub>2</sub> *6H <sub>2</sub> O	0.02
CoSO <sub>4</sub> *5H <sub>2</sub> O	0.56



## References

- [1] Geneious prime® 2019.2.3.
- [2] E. Alani, L. Cao, and N. Kleckner. A method for gene disruption that allows repeated use of URA3 selection in the construction of multiply disrupted yeast strains. *Genetics*, 116(4):541–545, aug 1987.
- [3] Johnson-A. Lewis J. Raff M. Roberts K. Alberts, B. and P. Walter. *Molecular biology of the cell*. Number 4. Wiley, 5th edition edition, jul 2008.
- [4] K E Allen, M T McNally, H S Lowendorf, C W Slayman, and S J Free. Deoxyglucose-resistant mutants of neurospora crassa: isolation, mapping, and biochemical characterization. *Journal of Bacteriology*, 171(1):53–58, 1989.
- [5] Takayuki Arazoe, Kennosuke Miyoshi, Tohru Yamato, Tetsuo Ogawa, Shuichi Ohsato, Tsutomu Arie, and Shigeru Kuwata. Tailor-made CRISPR/cas system for highly efficient targeted gene replacement in the rice blast fungus. *Biotechnology and Bioengineering*, 112(12):2543–2549, jul 2015.
- [6] Geraldine A. Auwera, Mauricio O. Carneiro, Christopher Hartl, Ryan Poplin, Guillermo del Angel, Ami Levy-Moonshine, Tadeusz Jordan, Khalid Shakir, David Roazen, Joel Thibault, Eric Banks, Kiran V. Garimella, David Altshuler, Stacey Gabriel, and Mark A. DePristo. From fastq data to high-confidence variant calls: The genome analysis toolkit best practices pipeline. *Current Protocols in Bioinformatics*, 43(1), oct 2013.
- [7] Sylvain Billiard, Manuela López-Villavicencio, Benjamin Devier, Michael E. Hood, Cécile Fairhead, and Tatiana Giraud. Having sex, yes, but with whom? inferences from fungi on the evolution of anisogamy and mating types. *Biological Reviews*, 86(2):421–442, aug 2010.
- [8] Andrew Carroll and Chris Somerville. Cellulosic biofuels. *Annual Review of Plant Biology*, 60(1):165–182, jun 2009.
- [9] Carmen de Sena-Tomás, Eun Young Yu, Arturo Calzada, William K. Holloman, Neal F. Lue, and José Pérez-Martín. Fungal ku prevents permanent cell cycle arrest by suppressing DNA damage signaling at telomeres. *Nucleic Acids Research*, 43(4):2138–2151, feb 2015.
- [10] Huaxiang Deng, Ruijie Gao, Xiangru Liao, and Yujie Cai. CRISPR system in filamentous fungi: Current achievements and future directions. *Gene*, 627:212–221, sep 2017.
- [11] Maria Dimarogona, Evangelos Topakas, and Paul Christakopoulos. Cellulose degradation by

- oxidative enzymes. *Computational and Structural Biotechnology Journal*, 2(3):e201209015, sep 2012.
- [12] Jennifer A. Doudna and Emmanuelle Charpentier. The new frontier of genome engineering with CRISPR-cas9. *Science*, 346(6213):1258096, nov 2014.
- [13] Zarah Forsberg, Morten Sørli, Dejan Petrović, Gaston Courtade, Finn L Aachmann, Gustav Vaae-Kolstad, Bastien Bissaro, Åsmund K Røhr, and Vincent GH Eijsink. Polysaccharide degradation by lytic polysaccharide monoxygenases. *Current Opinion in Structural Biology*, 59:54–64, dec 2019.
- [14] Andrew J. Foster, Magdalena Martin-Urdiroz, Xia Yan, Harriet Sabrina Wright, Darren M. Soanes, and Nicholas J. Talbot. CRISPR-cas9 ribonucleoprotein-mediated co-editing and counterselection in the rice blast fungus. *Scientific Reports*, 8(1), sep 2018.
- [15] Mónica Gandía, Shaomei Xu, Cristina Font, and Jose F. Marcos. Disruption of ku70 involved in non-homologous end-joining facilitates homologous recombination but increases temperature sensitivity in the phytopathogenic fungus *penicillium digitatum*. *Fungal Biology*, 120(3):317–323, mar 2016.
- [16] S. B. Gelvin. Agrobacterium-mediated plant transformation: the biology behind the "gene-jockeying" tool. *Microbiology and Molecular Biology Reviews*, 67(1):16–37, mar 2003.
- [17] Maximilian Haeussler, Kai Schönig, Hélène Eckert, Alexis Eschstruth, Joffrey Mianné, Jean-Baptiste Renaud, Sylvie Schneider-Maunoury, Alena Shkumatava, Lydia Teboul, Jim Kent, Jean-Stephane Joly, and Jean-Paul Concordet. Evaluation of off-target and on-target scoring algorithms and integration into the guide RNA selection tool CRISPOR. *Genome Biology*, 17(1), jul 2016.
- [18] B. Hahn-Hägerdal, M. Galbe, M.F. Gorwa-Grauslund, G. Lidén, and G. Zacchi. Bio-ethanol – the fuel of tomorrow from the residues of today. *Trends in Biotechnology*, 24(12):549–556, dec 2006.
- [19] Renate Heinzlmann, Daniel Croll, Stefan Zoller, György Sipos, Martin Münsterkötter, Ulrich Güldener, and Daniel Rigling. High-density genetic mapping identifies the genetic basis of a natural colony morphology mutant in the root rot pathogen *armillaria ostoyae*. *Fungal Genetics and Biology*, 108:44–54, nov 2017.
- [20] Nathan J. Hillson, Rafael D. Rosengarten, and Jay D. Keasling. j5 DNA assembly design automation software. *ACS Synthetic Biology*, 1(1):14–21, dec 2011.

- [21] Paul J. J. Hooykaas, G. Paul H. van Heusden, Xiaolei Niu, M. Reza Roushan, Jalal Soltani, Xiaorong Zhang, and Bert J. van der Zaal. Agrobacterium-mediated transformation of yeast and fungi. In *Current Topics in Microbiology and Immunology*, pages 349–374. Springer International Publishing, 2018.
- [22] Lori B. Huberman, Jason Liu, Lina Qin, and N. Louise Glass. Regulation of the lignocellulolytic response in filamentous fungi. *Fungal Biology Reviews*, 30(3):101–111, jul 2016.
- [23] Jake Z. Jacobs, Keith M. Ciccaglione, Vincent Tournier, and Mikel Zaratiegui. Implementation of the CRISPR-cas9 system in fission yeast. *Nature Communications*, 5(1), oct 2014.
- [24] Daehwan Kim. Physico-chemical conversion of lignocellulose: Inhibitor effects and detoxification strategies: A mini review. *Molecules*, 23(2):309, feb 2018.
- [25] H. Li and R. Durbin. Fast and accurate short read alignment with burrows-wheeler transform. *Bioinformatics*, 25(14):1754–1760, may 2009.
- [26] Zhonghai Li, Guangshan Yao, Ruimei Wu, Liwei Gao, Qinbiao Kan, Meng Liu, Piao Yang, Guodong Liu, Yuqi Qin, Xin Song, Yaohua Zhong, Xu Fang, and Yinbo Qu. Synergistic and dose-controlled regulation of cellulase gene expression in penicillium oxalicum. *PLOS Genetics*, 11(9):e1005509, sep 2015.
- [27] Lee R Lynd. The grand challenge of cellulosic biofuels. *Nature Biotechnology*, 35(10):912–915, oct 2017.
- [28] Shara D McClendon, Tanveer Batth, Christopher J Petzold, Paul D Adams, Blake A Simmons, and Steven W Singer. *Thermoascus aurantiacus* is a promising source of enzymes for biomass deconstruction under thermophilic conditions. *Biotechnology for Biofuels*, 5(1):54, 2012.
- [29] Robert L. Metzenberg. Vogel's medium n salts: avoiding the need for ammonium nitrate. *Fungal Genetics Reports*, 50(1):14–14, dec 2003.
- [30] Caroline B. Michielse, Paul J. J. Hooykaas, Cees A. M. J. J. van den Hondel, and Arthur F. J. Ram. Agrobacterium-mediated transformation as a tool for functional genomics in fungi. *Current Genetics*, 48(1):1–17, may 2005.
- [31] Min Ni, Marianna Feretzaki, Sheng Sun, Xuying Wang, and Joseph Heitman. Sex in fungi. *Annual Review of Genetics*, 45(1):405–430, dec 2011.

- [32] Christina S. Nødvig, Jakob B. Hoof, Martin E. Kogle, Zofia D. Jarczynska, Jan Lehmbeck, Dorte K. Klitgaard, and Uffe H. Mortensen. Efficient oligo nucleotide mediated CRISPR-cas9 gene editing in aspergilli. *Fungal Genetics and Biology*, 115:78–89, jun 2018.
- [33] Christina S. Nødvig, Jakob B. Nielsen, Martin E. Kogle, and Uffe H. Mortensen. A CRISPR-cas9 system for genetic engineering of filamentous fungi. *PLOS ONE*, 10(7):e0133085, jul 2015.
- [34] Intergovernmental Panel on Climate Change. *Climate Change 2014: Mitigation of Climate Change*. Cambridge University Press, 2015.
- [35] Nicholas R. Pannunzio, Go Watanabe, and Michael R. Lieber. Nonhomologous DNA end-joining for repair of DNA double-strand breaks. *Journal of Biological Chemistry*, 293(27):10512–10523, dec 2017.
- [36] Henrique Cestari De Paoli, Gerald A. Tuskan, and Xiaohan Yang. An innovative platform for quick and flexible joining of assorted DNA fragments. *Scientific Reports*, 6(1), jan 2016.
- [37] Steven T Pullan, Paul Daly, Stéphane Delmas, Roger Ibbett, Matthew Kokolski, Almar Neiteler, Jolanda M van Munster, Raymond Wilson, Martin J Blythe, Sanyasi Gaddipati, Gregory A Tucker, and David B Archer. RNA-sequencing reveals the complexities of the transcriptional response to lignocellulosic biofuel substrates in aspergillus niger. *Fungal Biology and Biotechnology*, 1(1), nov 2014.
- [38] Katarzyna Robak, , and Maria Balcerek. Review of second-generation bioethanol production from residual biomass. *Food Technology and Biotechnology*, 56(2), 2018.
- [39] Timo Schuerg, Raphael Gabriel, Nora Baecker, Scott E. Baker, and Steven W. Singer. *Thermoascus aurantiacus* is an intriguing host for the industrial production of cellulases. *Current Biotechnology*, 6(2):89–97, apr 2017.
- [40] Timo Schuerg, Jan-Philip Prah, Raphael Gabriel, Simon Harth, Firehiwot Tachea, Chyi-Shin Chen, Matthew Miller, Fabrice Masson, Qian He, Sarah Brown, Mona Mirshiaghi, Ling Liang, Lauren M. Tom, Deepti Tanjore, Ning Sun, Todd R. Pray, and Steven W. Singer. Xylose induces cellulase production in *thermoascus aurantiacus*. *Biotechnology for Biofuels*, 10(1), nov 2017.
- [41] Kerstin Schultenkämper, Luciana F. Brito, and Volker F. Wendisch. Impact of CRISPR interference on strain development in biotechnology. *Biotechnology and Applied Biochemistry*, 67(1):7–21, jan 2020.

- [42] Insightful Science. Snapgene software.
- [43] Bernhard Seiboth, Christa Ivanova, and Verena Seidl-Seiboth. Trichoderma reesei: A fungal enzyme producer for cellulosic biofuels. In *Biofuel Production-Recent Developments and Prospects*. InTech, sep 2011.
- [44] V. Seidl, C. Seibel, C. P. Kubicek, and M. Schmoll. Sexual development in the industrial workhorse trichoderma reesei. *Proceedings of the National Academy of Sciences*, 106(33):13909–13914, aug 2009.
- [45] Océane Seudre, Alice Namias, Olivia Gardella, Guillaume Da Silva, Pierre-Henri Gouyon, and Manuela López-Villavicencio. Why outcross? the abandon-ship hypothesis in a facultative outcrossing/selfing fungal species. *Fungal Genetics and Biology*, 120:1–8, nov 2018.
- [46] Tian-Qiong Shi, Guan-Nan Liu, Rong-Yu Ji, Kun Shi, Ping Song, Lu-Jing Ren, He Huang, and Xiao-Jun Ji. CRISPR/cas9-based genome editing of the filamentous fungi: the state of the art. *Applied Microbiology and Biotechnology*, 101(20):7435–7443, sep 2017.
- [47] Daniel Solis-Escalante, Niels G.A. Kuijpers, Nadine Bongaerts, Irina Bolat, Lizanne Bosman, Jack T. Pronk, Jean-Marc Daran, and Pascale Daran-Lapujade. amdSYM, a new dominant recyclable marker cassette for *Saccharomyces cerevisiae*. *FEMS Yeast Research*, 13(1):126–139, feb 2013.
- [48] Runjie Song, Qing Zhai, Lu Sun, Enxia Huang, Yu Zhang, Yanli Zhu, Qingyun Guo, Yanan Tian, Baoyu Zhao, and Hao Lu. CRISPR/cas9 genome editing technology in filamentous fungi: progress and perspective. *Applied Microbiology and Biotechnology*, 103(17):6919–6932, jul 2019.
- [49] Hans Visser, Vivi Joosten, Peter J. Punt, Alexander V. Gusakov, Phil T. Olson, Rob Joosten, Jeffrey Bartels, Jaap Visser, Arkady P. Sinitsyn, Mark A. Emalfarb, Jan C. Verdoes, and Jan Wery. RESEARCH: Development of a mature fungal technology and production platform for industrial enzymes based on a *myceliophthora thermophila* isolate, previously known as *chrysosporium lucknowense* c1. *Industrial Biotechnology*, 7(3):214–223, jun 2011.
- [50] Lauren Wensing, Jehoshua Sharma, Deeva Uthayakumar, Yannic Proteau, Alejandro Chavez, and Rebecca S. Shapiro. A CRISPR interference platform for efficient genetic repression in *Candida albicans*. *mSphere*, 4(1), feb 2019.

- [51] Guangshan Yao, Zhonghai Li, Liwei Gao, Ruimei Wu, Qinbiao Kan, Guodong Liu, and Yinbo Qu. Redesigning the regulatory pathway to enhance cellulase production in penicillium oxalicum. *Biotechnology for Biofuels*, 8(1), apr 2015.

## List of Figures

2.1	Schema for the general production of biofuels from lignocellulosic biomass . . . .	3
2.2	Schema for cellulose degradation . . . . .	5
2.3	<i>T. aurantiacus</i> spores . . . . .	8
2.4	Schema for <i>Agrobacterium</i> Transformation . . . . .	9
2.5	Schema of a targeted gene knockout and selection on FAA, utilizing <i>amdS</i> as a recyclable marker . . . . .	10
2.6	Schema for the CRISPR-Cas9 system . . . . .	13
3.1	Cloning Strategy . . . . .	20
4.1	Sequencing results of putative carbon catabolite derepressed strains isolated from random mutagenesis mapped to the reference <i>creA</i> gene . . . . .	25
4.2	Sequencing results of selected $\Delta amdS$ mutants isolated from random mutagenesis mapped to the reference <i>amdS</i> gene . . . . .	25
4.3	Verification of the crossed progeny of $\Delta ku70$ and $\Delta pyrE$ . . . . .	26
4.4	Sequenced <i>pyrG</i> of the $\Delta ku70$ strains . . . . .	27
4.5	Crossing of a $\Delta amdS$ strains generated by random mutagenesis and TA wt . . .	28
4.6	Growth of putative <i>creA</i> mutants on 0.1% DOG . . . . .	31
4.7	Sequencing results for <i>creA</i> of selected strains that indicated a distorted CCR from the transformation with pJP6 or pJP7. . . . .	32
4.8	Growth of TA wt on minimal media with different carbon sources . . . . .	33
4.9	Growth of putative <i>creA</i> deletion mutants on minimal media with DOG . . . .	34
4.10	Sequencing results for <i>creA</i> of the thought to be $\Delta creA$ strains show a functional gene . . . . .	34
7.1	L0 gRNA plasmid . . . . .	46
7.2	Schema of Golden Gate Cloning . . . . .	46
7.3	Bpi1 KO plasmid . . . . .	47
7.4	CRISPR/Cas9 Knockout Plasmid . . . . .	48
7.5	AB3996 Plasmid . . . . .	49

## List of Tables

4.1	Targeted genes and the used plasmids in the CRISPR-Cas9 experiments . . . . .	29
4.2	SNPs in the Bpi1 KO plasmid . . . . .	30
7.1	List of all abbreviations used . . . . .	43
7.2	All assembled plasmids . . . . .	50
7.3	Liquid induction media . . . . .	52
7.4	Solid induction media . . . . .	52
7.5	20X AB salt solution . . . . .	53
7.6	500 mM phosphate solution . . . . .	53
7.7	MES buffer . . . . .	53
7.8	DNS reagent . . . . .	53
7.9	McClendon's media component I . . . . .	54
7.10	McClendon's salts A . . . . .	54
7.11	McClendon's salts B . . . . .	54
7.12	McClendon's trace elements . . . . .	54